MICROCOPY RESOLUTION TEST CHART

NATIONAL BUREAU OF STANDARDS-1963-A

AD-A181713

REPORT DOCUMENTATION PAGE		Form Approved OMB No 0704 0188 Exp Date Jun 30 1986

1a. REPORT SECURITY CLASSIFICATION Unclassified	1b RESTRICTIVE MARKINGS

2a. SECURITY CLASSIFICATION AUTHORITY	3 DISTRIBUTION / AVAILABILITY OF REPORT Approved for public release; distribution unlimited
2b. DECLASSIFICATION / DOWNGRADING SCHEDULE	

4 PERFORMING ORGANIZATION REPORT NUMBER(S) Technical Report ITL-87-1	5 MONITORING ORGANIZATION REPORT NUMBER(S)

6a. NAME OF PERFORMING ORGANIZATION Department of Civil Engineering	6b OFFICE SYMBOL (If applicable)	7a NAME OF MONITORING ORGANIZATION

6c. ADDRESS (City, State, and ZIP Code) The University of Toledo 2801 Bancroft Street West Toledo, Ohio 43606	7b ADDRESS (City, State, and ZIP Code)

8a. NAME OF FUNDING / SPONSORING ORGANIZATION See reverse	8b OFFICE SYMBOL (If applicable)	9 PROCUREMENT INSTRUMENT IDENTIFICATION NUMBER

8c. ADDRESS (City, State, and ZIP Code) See reverse	10 SOURCE OF FUNDING NUMBERS See reverse			
	PROGRAM ELEMENT NO	PROJECT NO	TASK NO	WORK UNIT ACCESSION NO

11 TITLE (Include Security Classification) Recommendations: Load-Transfer Criteria for Piles in Clay

12 PERSONAL AUTHOR(S) Andrew G. Heydinger

13a. TYPE OF REPORT Final Report	13b TIME COVERED FROM _____ TO _____	14 DATE OF REPORT (Year, Month, Day) January 1987	15 PAGE COUNT 82

16 SUPPLEMENTARY NOTATION Available from National Technical Information Service, 5285 Port Royal Road, Springfield, Virginia 22161.

17	COSATI CODES		18 SUBJECT TERMS (Continue on reverse if necessary and identify by block number)
FIELD	GROUP	SUB-GROUP	Axial loads Piles (Civil engineering) Clay Foundations

19 ABSTRACT (Continue on reverse if necessary and identify by block number)

This report presents a comprehensive evaluation of load-transfer criteria for analysis of axially loaded piles in clay. The US Army Corps of Engineers installs thousands of piles each year in the construction of navigational and flood control structures. So that these structures will perform satisfactorily, not only must the capacity of the pile foundations be adequately determined but the load-deformation behavior of the foundation must also be predicted to allow an analysis of the structure for stresses and deformations. Various predictive methods for computing side resistance capacity and shear transfer versus vertical pile movement, f-z curves, for clay are presented. Parametric studies were conducted to determine the method that could best represent pile behavior. Instrumented pile loads were used to evaluate the performance of the methods under actual field conditions. Based on these investigations, procedures for determining side resistance and shear transfer versus vertical pile movement are recommended. Keywords for Structures, Structural foundations, Axial loads. ▲

20 DISTRIBUTION / AVAILABILITY OF ABSTRACT ☑ UNCLASSIFIED/UNLIMITED ☐ SAME AS RPT ☐ DTIC USERS	21 ABSTRACT SECURITY CLASSIFICATION Unclassified
22a NAME OF RESPONSIBLE INDIVIDUAL	22b TELEPHONE (Include Area Code)	22c OFFICE SYMBOL

DD FORM 1473, 84 MAR   83 APR edition may be used until exhausted   SECURITY CLASSIFICATION OF THIS PAGE
                               All other editions are obsolete

8a. NAME OF FUNDING/SPONSORING ORGANIZATION (Continued).

Information Technology Laboratory, US Army Engineer Waterways Experiment Station and US Army Engineer Division, Lower Mississippi Valley Division.

8c. ADDRESS (Continued).

PO Box 631, Vicksburg, MS 39180-0631
and PO Box 80, Vicksburg, MS 39180-0080

10. SOURCE OF FUNDING NUMBERS (Continued).

DACW39-84-M-2309

PREFACE

This report presents criteria for load-transfer and numerical analysis of axially loaded piles in clay. These criteria were selected from the latest published information on axially loaded piles in clay and reflect the current state-of-the-art in pile foundation.

Dr. Andrew G. Heydinger, Department of Civil Engineering, The University of Toledo, Toledo, Ohio, prepared the report under Contract No. DACW39-84-M-2309. The work in developing these criteria was done as part of the application support provided by the Information Technology Laboratory (ITL), formerly Automation Technology Center (ATC), US Army Engineer Waterways Experiment Station (WES), to the US Army Engineer Division, Lower Mississippi Valley (LMVD). The point of contact for LMVD was Mr. James A. Young.

At WES the coordination and monitoring was accomplished by Mr. Reed Mosher, Engineering Application Group, formerly of Scientific and Engineering Application Division (SEAD), ATC. Mr. Mosher provided technical guidance and review on the project under the general supervision of Mr. Paul K. Senter, Acting Chief, Information Research Division (formerly SEAD), and Dr. N. Radhakrishnan, Acting Chief, ITL, formerly Chief ATC, WES. Information Products Division, ITL, WES, Editor and Editorial Assistant Mses. Gilda Shurden and Frances Williams, respectively, prepared the report for publication.

COL Allen F. Grum, USA, was the previous Director of WES. COL Dwayne G. Lee, CE, is the present Commander and Director. Dr. Robert W. Whalin is Technical Director.

Accesion For		
NTIS CRA&I	☑	
DTIC TAB	☐	
U.announced	☐	
Justification		
By		
Distribution /		
Availability Codes		
Dist	Avail a: d/or Special	
A-1		

1

CONTENTS

CONVERSION FACTORS, NON-SI TO SI (METRIC)
UNITS OF MEASUREMENT

Non-SI units of measurement used in this report can be converted to SI (metric) units as follows:

Multiply	By	To Obtain
feet	0.3048	metres
inches	0.0254	metres
kips (force) per square foot	47.88026	kilopascals
pounds	4.448222	newtons
pounds (force) per square foot	47.88026	pascals
pounds (mass) per cubic foot	16.01846	kilograms per cubic metre
pounds (force) per square inch	6.894757	kilopascals
tons (force)	8.896444	kilonewtons

RECOMMENDATIONS: LOAD-TRANSFER
CRITERIA FOR PILES IN CLAY

PART I: INTRODUCTION

Background

1. The US Army Corps of Engineers (CE) designs and/or oversees the de-
sign of many structures with pile foundations in cohesive soils. So that
these structures will perform satisfactorily, not only the capacity of the
foundations must be adequate but also the load-deformation behavior of the
foundations must be predicted to allow an analysis of the structures for
stresses and deformations. The difficult task of structure analysis is accom-
plished with the aid of computer programs which rely on input on the founda-
tion behavior. The information in this report is intended to form the back-
ground for developing a computer subroutine to generate data to create design
charts for piles in cohesive soils or a subroutine in a large interactive
program for pile design.

2. The capacity of a foundation is measured by its ability to withstand
loads without excessive settlements. The capacity of piles in clay consists
of the resistance to penetration at the tip of the piles and the side-shear
resistance. A solution requires identification of pertinent soils properties
and the resulting conditions after the piles have been installed.

3. The load-deformation behavior of piles, the predicted settlements,
and their respective loads require determination of functions for pile-soil
interaction behavior. The functions define the dependence of side or tip re-
sistance on vertical pile movements. Computer programs have been developed at
the US Army Engineer Waterways Experiment Station (WES) (Radhakrishnan and
Parker 1975) to make use of recommended procedures for predicting pile-soil
interaction. However, problems associated with predicting behavior are more
complex than the initial procedures can account for, so this research was
necessary.

4. For the purpose of foundation design, soils can be classified as co-
hesive or cohesionless. Cohesive soils are fine-grained soils with low perme-
abilities and shear strengths with a dependence on attractive forces between

4

the soil particles. Cohesionless soils are coarse-grained soils with high permeabilities and shear strengths and a dependence on the stresses acting on the soil particles. Problems associated with piles in cohesionless soils have recently been addressed by Mosher (1984). Large pore pressures and severe soil remolding occur during pile installation in cohesive soils, resulting in problems unique from those of cohesionless soils. Such problems are considered in this report.

Purpose

5. Investigation of design procedures for axially loaded single piles in cohesive soils and recommendations for their use are the purpose of this research project. More specifically, predictive methods for computing capacity and shear transfer versus vertical pile movement, f-z* curves, were investigated. The specific objective for this research was to investigate piles of 100 ft** or less in length, and precast concrete piles and H-piles that are likely to be used on CE projects. Additionally, this research includes information and recommendations for estimating soil properties that are useful for the design of piles.

Scope

6. This report includes research on proposed predictive methods for axial capacity and on the effects of pile installation on soil properties. The study includes the most recent attempts to determine the changes in shear strength and the state of stress around piles in clay. The predictive methods that are discussed are total stress methods based on in situ (before pile installation) soil properties and effective stress methods.

7. Research on load-deformation behavior is directed toward determining f-z curves, which can be used in a WES program to compute pile behavior. Four proposed methods were analyzed to determine a recommended method for CE purposes. Parametric studies were conducted to determine the method that

---

* For convenience, symbols and abbreviations are listed in the notation (Appendix A).
** A table of factors for converting non-SI units of measurement to SI (metric) units is presented on page 3.

could best be used to represent actual soil conditions. Results of four instrumented pile-load tests were also used to evaluate the methods.

8. Research on soil properties consists of correlations that can be used to determine in situ soil properties. The research includes correlations for the undrained shear strength, the effective friction angle, K_o, and Young's modulus. The correlations can be used for designing piles.

PART II: CAPACITY OF PILES IN COHESIVE SOILS

Introduction

9. Methods to compute pile capacity are referred to as total or effective stress methods. Total stress methods rely on in situ soil properties or stresses and empirical observations obtained from pile load tests. Three methods that have been used are the α-method (American Petroleum Institute (API) 1978, Vesic 1972), the β-method (Meyerhof 1976), and the λ-method (Vijayvergiya and Focht 1972). Effective stress methods are based on predictions of the effective stresses in the soil around piles in clay at the time of loading. The methods are those reported by Esrig and Kirby (1979), Kraft (1982), and Heydinger and O'Neill (in preparation). This section reviews information on the predictive methods and determines a recommended design procedure for CE projects.

10. Error can occur with these predictive methods from a number of sources. For piles, the pile material and the method of installation affect the results. For pile testing, there are differences in the way and the rate that the loads are applied. Error also occurs in measuring the applied loads, particularly if load cells are not used. For soils, different methods have been used to obtain the undrained shear strengths. There is considerable variation in soil properties for a given site, requiring estimation of the undrained shear strength. Test results can be varied, depending on the length of time following installation. Excess pore pressures and reduced shear strengths exist for periods up to 30 days or longer.

Total Stress Methods

α-method

11. The α-method (API 1978, Vesic 1972) is based on observations that the ratio of the pile-soil adhesion, c_a , to the undrained shear strength of the soil decreases as the undrained shear strength increases. The ratio is a parameter α that is given as a function of the undrained shear strength. The total pile capacity, Q_u , is then computed by using Equation 1:

$$Q_u = \alpha s_u A_s + N_c s_u A_t \tag{1}$$

7

where

s_u = undrained shear strength along the side of the pile or at the pile tip

A_s = area of the pile surface equal to the perimeter of the pile multiplied by the pile length

N_c = cohesive bearing factor (for piles in clay, N_c can be taken as 9)

A_t = cross-sectional area of the pile tip

In practice, values of α have been computed using the averages of c_a and s_u for the total embedded lengths, and the side-frictional capacity is computed by dividing the subsurface into a number of layers using the average undrained shear strength of each layer.

12. There are factors that influence the accuracy of the α-method. Pile-soil adhesion is not only dependent on the undrained shear strength but is also dependent on the soil composition, stress history, and sensitivity. It has also been shown (Kraft, Focht, and Amarasinghe 1981) that there is also some dependence of adhesion on the depth of embedment and the soil stiffness rather than being limited to values prescribed by α .

13. In spite of these shortcomings, the α-method has been widely used and will continue to be used. More reliable results would be obtained if unpublished load-test results from short, onshore piles were analyzed. Other investigators (Dennis and Olson 1983) (Kraft, Focht, and Amarasinghe 1981) have conducted such studies for steel pipe piles for offshore purposes.

14. The literature contains a number of recommendations to obtain pile-soil adhesion, according to the α-method. Figure 1 from Tomlinson (1957) shows curves for adhesion as a function of shear strength. Table 1 contains values of adhesion recommended by Tomlinson (1964). Figure 2 from Vesic (1977) illustrates values of adhesion from a number of tests including tests on cast-in-place concrete piles. Figure 3 (Tomlinson 1971) gives adhesion factors for stiff clays for piles with a penetration ratio, depth of penetration in clay divided by pile diameter, greater than 20 for piles other than H-piles. A recommendation is to use $\alpha = 0.4$ for piles with a penetration ratio between 8 and 20. Figure 4 indicates recommendations by other researchers (Vesic 1977).

15. Results of statistical analyses by other researchers have been published recently. Kraft, Focht, and Amarasinghe (1981) analyzed the results of testing on closed and open-end pipe piles, timber, and concrete piles. Values
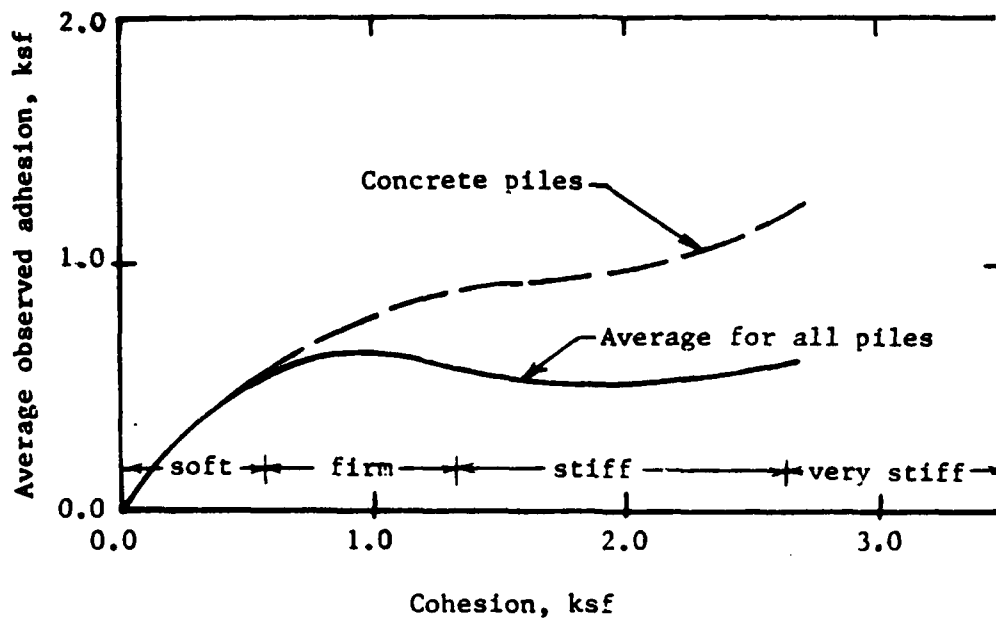
8

Figure 1.   Adhesion for soft to stiff clays (Tomlinson 1957)
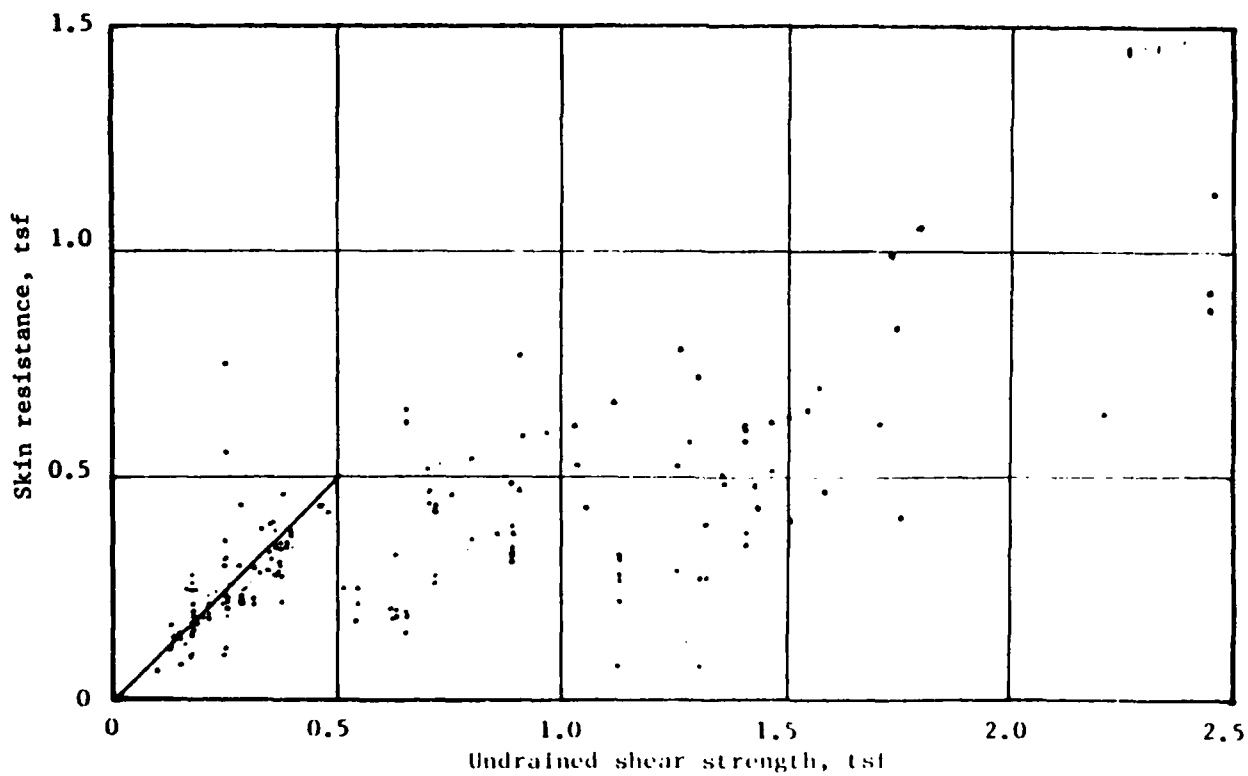
Figure 2.   Comparison of side resistance and undrained
shear strength (Vesic 1977)
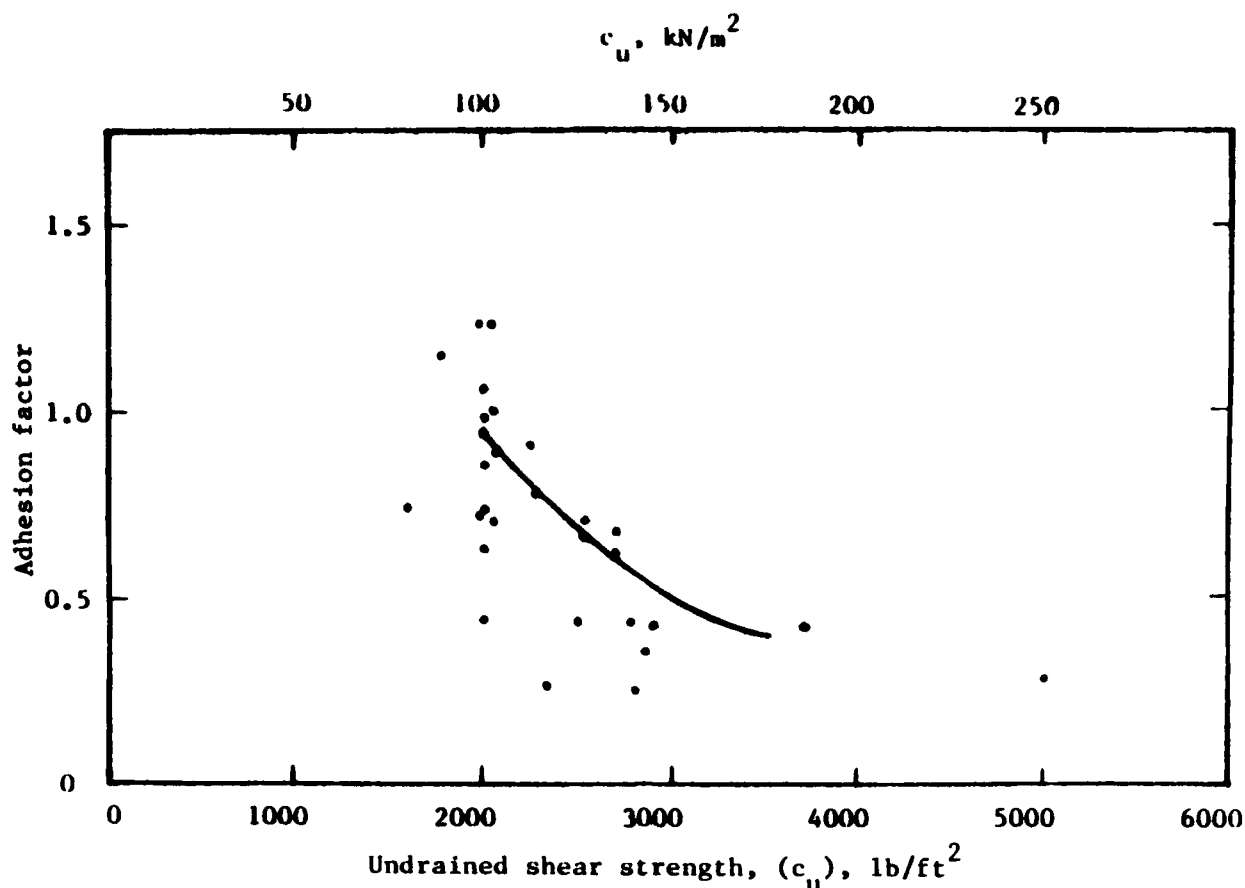
Figure 3. Adhesion factors for stiff clays (Tomlinson 1971)

of α were computed by a method proposed by the API (1978) and outlined as follows. For highly plastic clays with liquid limits and plasticity indices greater than 50 and 35 percent, respectively, $\alpha = 1$ except for overconsolidated clays where c_a must be less than 1 ksf or the undrained shear strength of the soil if it was normally consolidated clay, $(s_u)_{nc}$. For other clays, α varies linearly from 1 at $s_u = 0.5$ to 0.5 at $s_u = 1.5$ ksf.

16. Computed values of α were plotted as a function of pile length, L, and a parameter π_3 relating pile stiffness to soil stiffness.

$$\pi_3 = \pi D f_{max} \frac{L^2}{AE} u^*$$ (2)

where

D = pile diameter

f_{max} = maximum side resistance

A = cross-sectional area of the pile
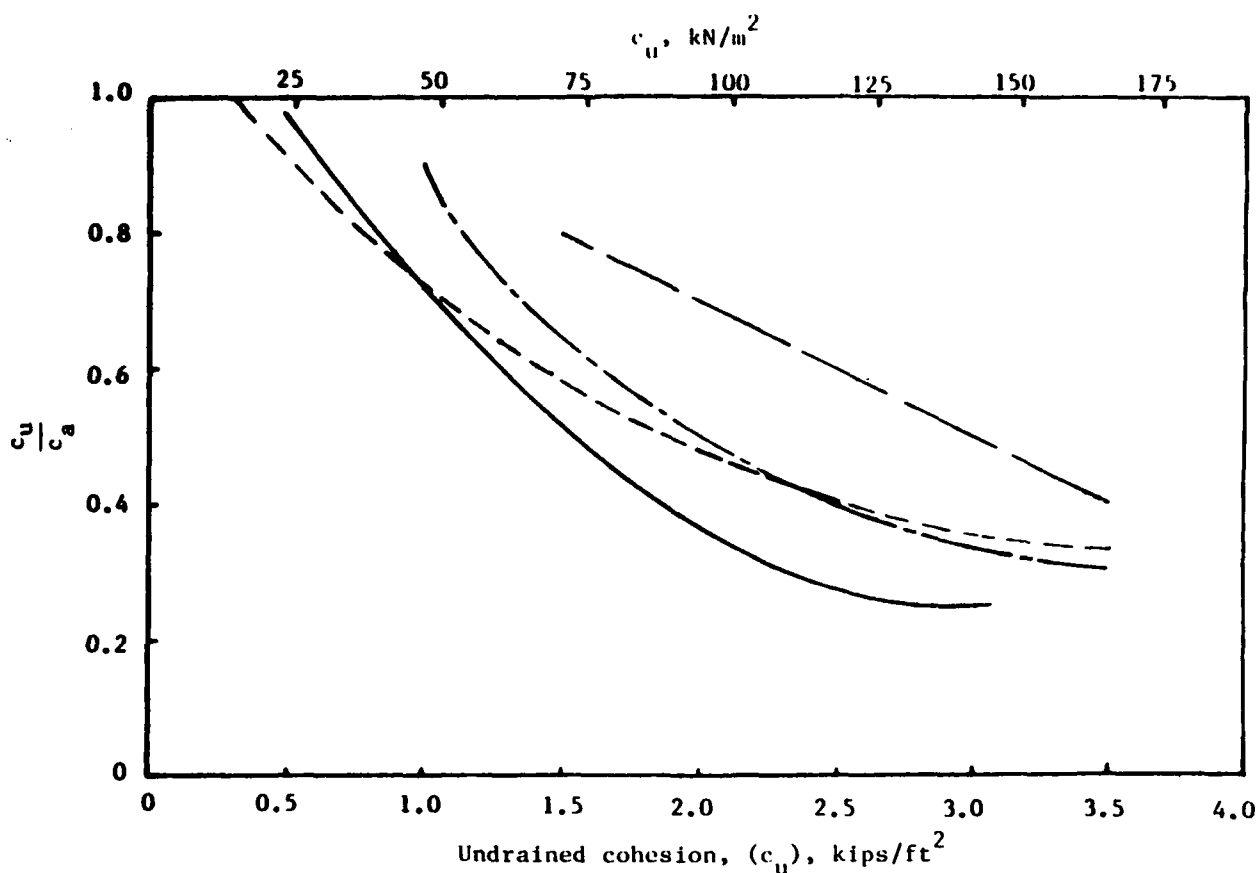
Figure 4. Adhesion factors for piles in clay (Vesic 1977)

E = Young's modulus of the pile

u^* = vertical pile movement at maximum side resistance

The relationships for α for normally consolidated soils are

$$\alpha = 1.486 - 0.126 \ln(L) \qquad (3)$$

$$\alpha = 1.024 - 0.070 \ln(\pi_3) \qquad (4)$$

Similar expressions were obtained for overconsolidated soils. The linear correlation coefficients are -0.27 and -0.33 for Equations 3 and 4, respectively. The authors also determined the ratios of computed to measured capacity. A mean of 1.10 and standard deviation of 0.34 was obtained by using Equation 3, and a mean of 1.09 and standard deviation of 0.31 was obtained by using Equation 4. So, in spite of the fact that the expressions do not correlate very well, reasonably accurate predictions of capacity can be made.

17. Predictions of capacity were obtained by using three diff~rent α-methods for steel pipe piles in normally or lightly overconsolidated clay (Gardner 1977). The first method used α as proposed by Tomlinson (1957) for steel piles. A second method for layered soil systems used values of α proposed by Tomlinson (1971), and the third is the method proposed by API (1978). Ratios of the computed to the measured capacities for 57 compression tests were calculated. The respective mean and standard deviations for the ratios were 0.74 and 0.48, 1.13 and 0.45, 1.07 and 0.37 for each of the three methods. A new method was proposed as follows:

$$Q_u = \alpha \bar{c}_u F_c F_L A_s + 9 c_u F_c A_t \tag{5}$$

where

$\bar{c}_u$ = average s_u

F_c = ratio of the undrained shear strength using unconsolidated undrained triaxial tests to the strengths obtained by other methods

F_L = 1.0 for lengths up to 100 ft and varies linearly to 1.8 at 175 ft

α = 1.0 for values of $\bar{c}_u F_c$ of 600 psf or less and varies linearly to 0.5 for $\bar{c}_u F_c$ equal to 1,200 psf and to 0.3 for $\bar{c}_u F_c$ equal to 5,000 psf

The mean for the ratios of computed to measured capacities was 1.00 and the standard deviation was 0.22.

18. In view of the previous discussion, the recommendation is to determine α according to the method proposed by Dennis and Olson (1983) for piles 100 ft or less. As shown in Figure 5, the recommendation for α is within the range of values of α that have been recommended by others. It is also recommended that the undrained shear strength be correlated to the unconsolidated-undrained triaxial strength. It is noted here that the use of Equations 3 and 4 could lead to overpredictions of capacity for piles less than 100 ft.

β-method

19. The β-method predicts the side resistance, f , as a function of the in situ vertical overburden pressure, σ'_{vo} .

$$f = \beta \sigma'_{vo} \le s_u \tag{6}$$
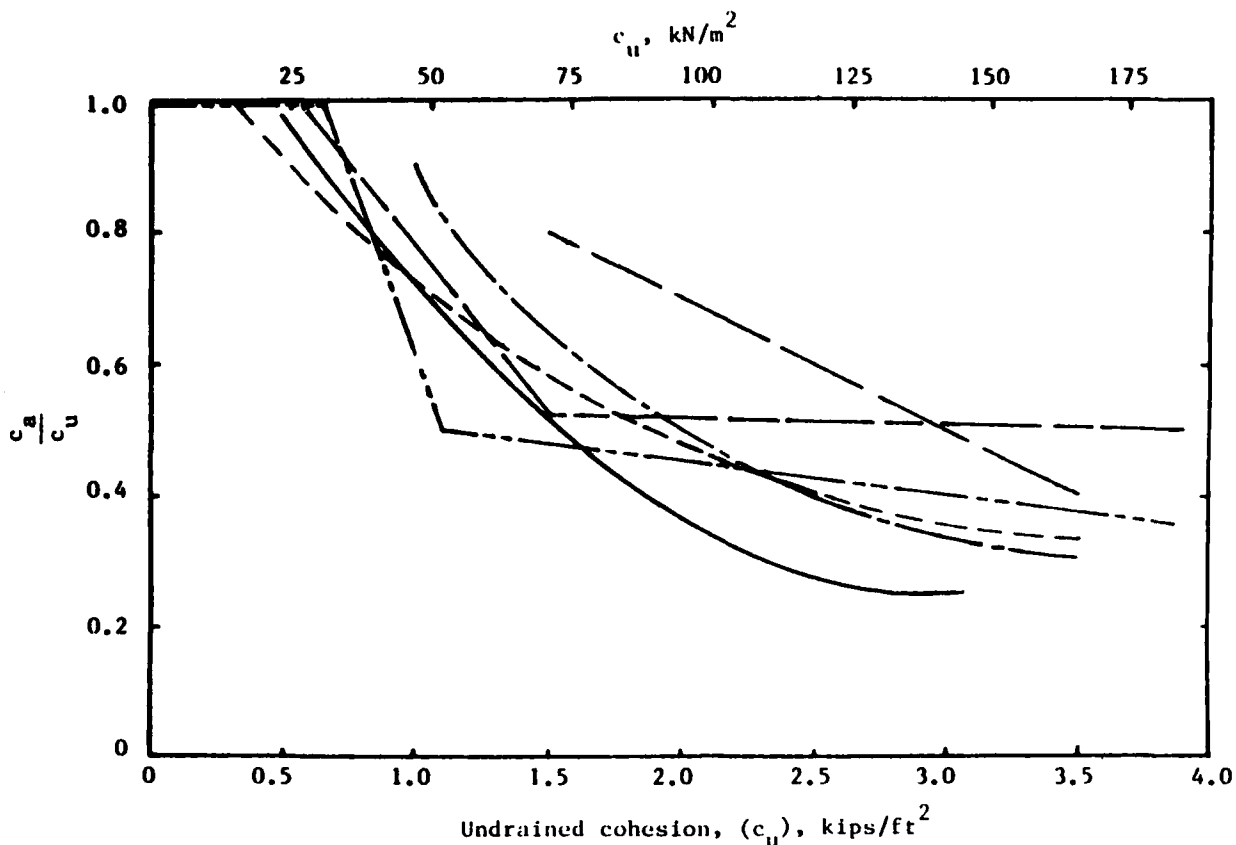
Figure 5. Adhesion factors as recommended by Dennis and Olson (1983)

pressure and the tangent of the effective angle of internal friction, ϕ' , as shown in Equation 7.

$$\beta = (1 - \sin \phi') \tan \phi' \ (OCR)^{1/2} \tag{7}$$

where OCR is the overconsolidation ratio. Another recommendation is to determine β as a function of pile length for normally and lightly overconsolidated clays. Figure 6 (Meyerhof 1976) indicates that the trend is for β to decrease with increasing pile length, particularly for piles longer than 100 ft. Meyerhof (1976) also recommends that β for overconsolidated soils be taken as

$$\beta = 1.5 \ (1 - \sin \phi') \tan \phi' \ (OCR)^{1/2} \tag{8}$$

20. Statistical analyses of the β-method were also presented by Kraft,

13

Figure 6. Skin friction factors for β
method (Meyerhof 1976)

Focht, and Amarasinghe (1981). The expressions for normally consolidated
soils are

$$\beta = 0.468 - 0.052 \ln(L) \qquad (9)$$

$$\beta = 0.0278 - 0.028 \ln(\pi_3) \tag{10}$$

The linear correlation coefficient for Equations 9 and 10 were -0.58 and -0.71, respectively. The respective mean and standard deviation of the ratio of computed to measured capacity were 1.05 and 0.22 for Equation 9, and 1.03 and 0.19 for Equation 10. Values of β did not correlate for overconsolidated soils. A recommendation for the use of the β-method is given subsequently.
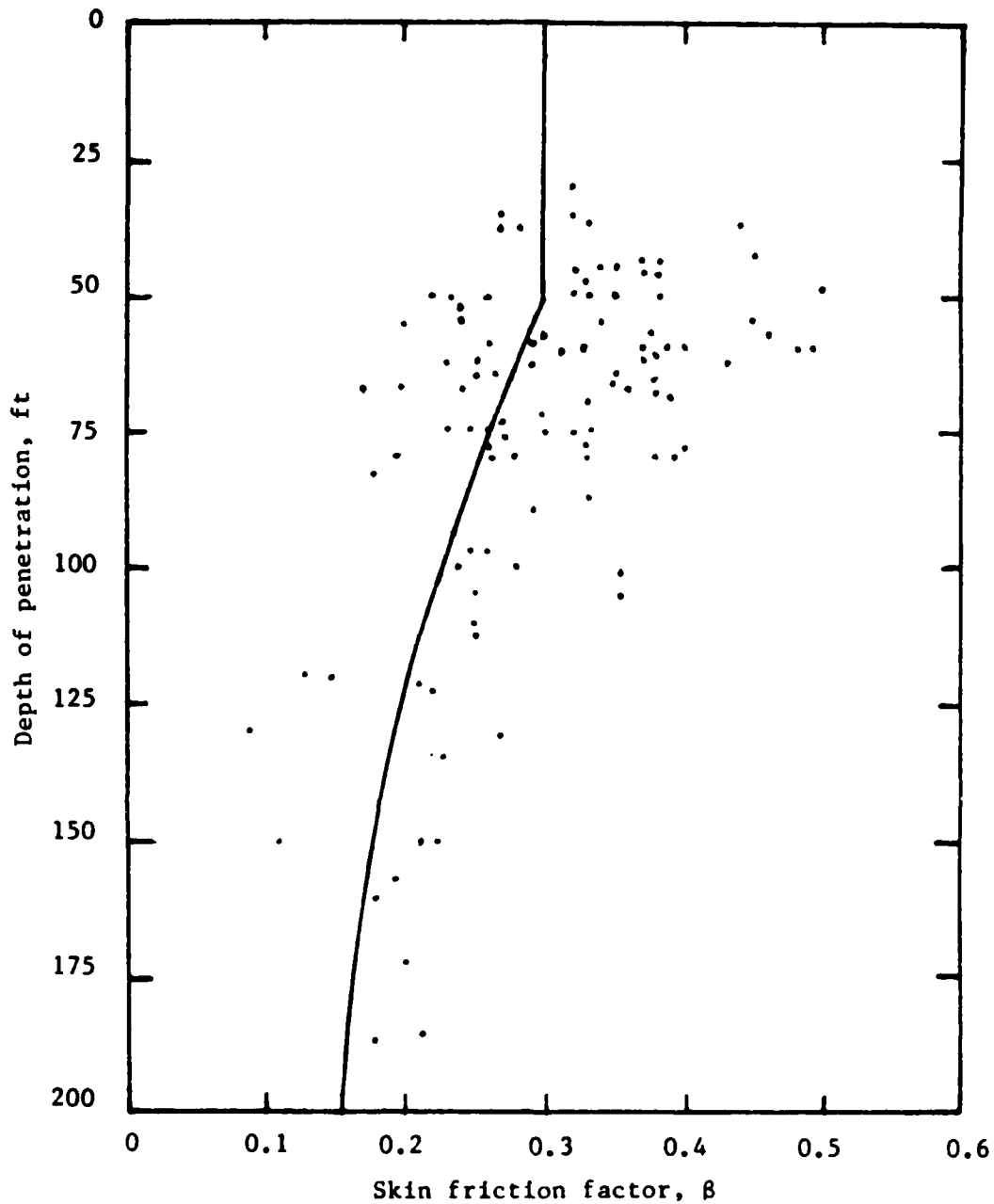
λ-method

21. The λ-method correlates the theoretical passive earth pressure to the side resistance (Vijayvergiya and Focht 1972).

$$f = \lambda(\sigma'_m + 2c_m) \tag{11}$$

where

σ'_m = mean, effective, overburden pressure

c_m = mean, undrained shear strength

both for the length of embedment. Figure 7 is a plot of λ versus pile length for pipe piles. The figure indicates that there is a strong correlation between the factor λ and pile embedment, that it decreases with length.

22. Results similar to the analyses of the previous two methods were also obtained for the λ-method. Kraft, Focht, and Amarasinghe (1981) determined relationships for λ as a function of pile length and π_3 for normally consolidated soils.

$$\lambda = 0.296 - 0.032 \ln(L) \tag{12}$$

$$\lambda = 0.178 - 0.016 \ln(\pi_3) \tag{13}$$

23. The expressions for overconsolidated soils, soils having ratios of the mean, undrained shear strength to the mean, effective, overburden pressure greater than 0.4, are

$$\lambda = 0.488 - 0.078 \ln(L) \tag{14}$$

$$\lambda = 0.232 - 0.032 \ln(\pi_3) \tag{15}$$

15
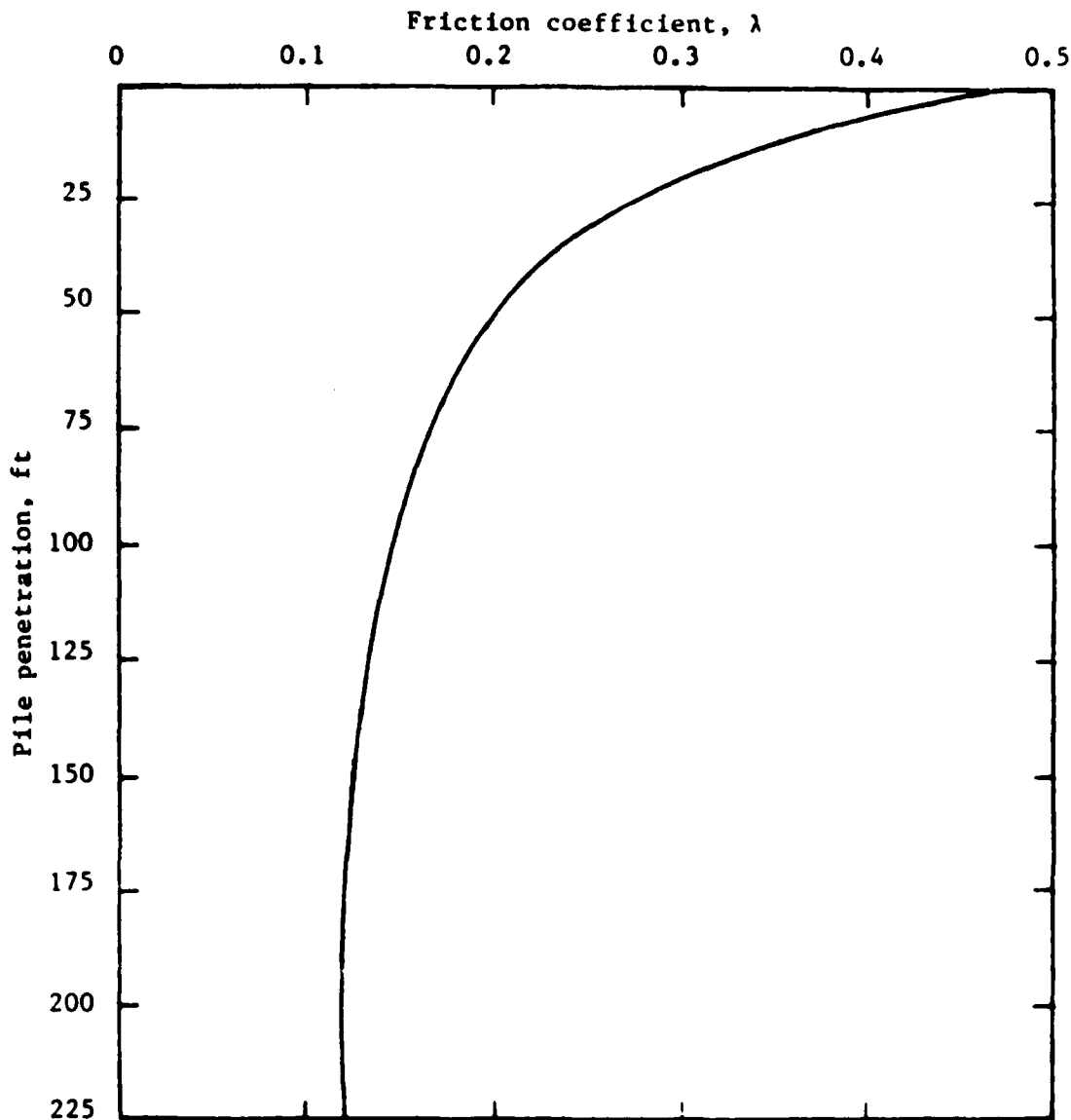
Figure 7. Correlation between λ and pile embedment (Vijayvergiya 1977a)

24. The linear correlation coefficients are -0.59, -0.68, -0.65, and -0.55 for Equations 12 through 15, respectively. The mean values of the ratios of the computed to measured capacities ranged from 1.06 to 1.09, and the standard deviations varied from 1.29 to 1.43. Very similar results were obtained by Dennis and Olsen (1983) in their analyses of the λ-method.

Comparison of three methods

25. It is possible to compare the three methods by plotting the recommended factors as a function of depth as per the β-method. The correlation

16

factor necessary is β_1 (Kraft, Focht, and Amarasinghe 1981) where

$$\beta_1 = \frac{s_u}{\sigma'_{vo}} \tag{16}$$

For the α-method and the λ-method, respectively, β then would be

$$\beta = \alpha\beta_1 \tag{17}$$

$$\beta = (1 + 2\beta_1) \tag{18}$$

Figure 8 shows a comparison of the three methods using $\beta_1 = 0.2$. The results obtained for the α-method and the λ-methods would result in lower predicted capacities in this particular case, but not for cases when $\beta_1 > 0.2$. The curves from the β-method represent mean values for soils for all values of β_1.

Effective Stress Methods

26. The development of various effective stress methods as a means of calculating pile capacity has occurred as a result of researchers' different attempts to calculate the state of stress in the soil around piles during loading. The state of stress is updated to represent conditions in the soil after pile installation, after soil consolidation, and at pile failure. Solutions require theoretical models to represent the strain behavior of soil that occurs during each of the conditions mentioned above, and a soil model to represent stress-strain-strength relationships. The accuracy of any effective stress method is, thus, dependent on the ability to model the strains that occur and the stress-strain behavior of the soil.

Modeling pile installation

27. Pile installation has been modeled using cylindrical cavity expansion (Esrig et al. 1977; Esrig and Kirby 1979; Heydinger and O'Neil, in preparation; Kirby, Esrig, and Murphy 1983; Kirby and Roussel 1979 and 1980; Kirby and Wroth 1977), or other equivalent methods (Carter, Randolph and Wroth 1979; Randolph, Carter, and Wroth 1979; Wroth, Carter, and Randolph, 1979). According to the methods, it is assumed that the soil only moves outward, radially (direction perpendicular to the pile surface), resulting in plane strain

17
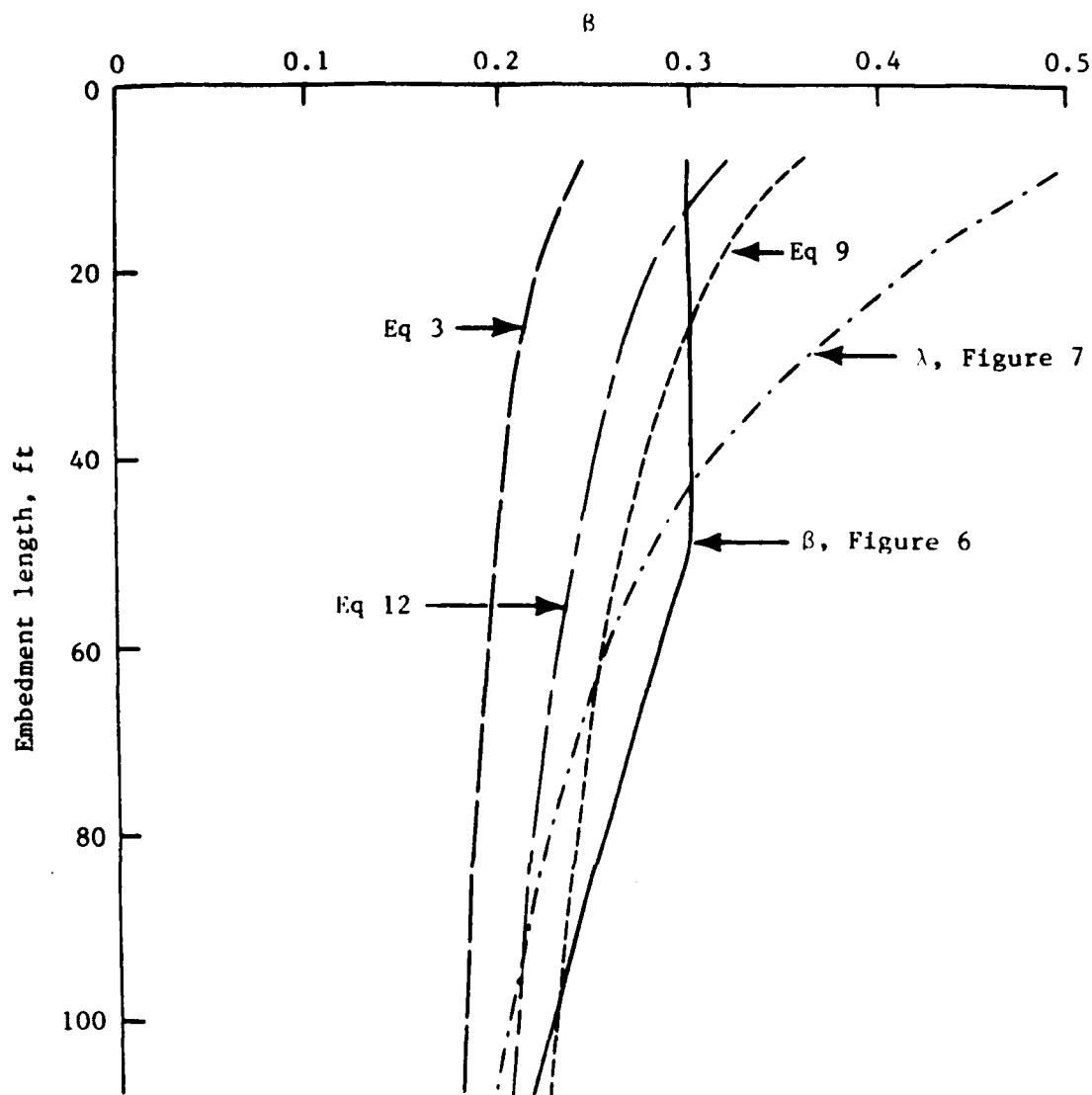
Figure 8. Comparison of predictive methods

conditions. For cylindrical cavity theory, the soil is assumed to behave as an elastic, perfectly plastic material. For the other formulations, work-hardening or softening effects can occur. Concepts of critical state soil mechanics (Kirby and Wroth 1977, Schofield and Wroth 1968) for soils at large strains are included in the models. Accordingly, soil reaches a unique relationship of stress-strain-volume that depends on the initial state of stress and strain and the stress history. The theories are used to compute the state of stress in the soil and the excess pore pressure distribution immediately following pile installation.

Modeling soil consolidation

28. Existing consolidation models assume that pore water movements occur only in the radial direction. Initially, it was assumed that the soil would remain at the critical state of effective stress during consolidation (Esrig et al. 1977, Kirby and Esrig 1979). Other solutions used an elastic soil model (Randolph and Wroth 1979), an elastic soil model with stiffness that increased with distance from the pile surface (Heydinger and O'Neill, in preparation; Leifer, Kirby, and Esrig 1979), an elasto-plastic soil model (Kavvadas and Baligh 1982; Miller, Murff, and Kraft 1978) and rigorous formulations that modeled the soil as an elasto-plastic material (Carter, Randolph, and Wroth 1979; Randolph, Carter, and Wroth 1979; Wroth, Carter, and Randolph 1979). Published results for the soil adjacent to the pile give the changes in mean effective stress or radial effective stress as a function of the excess pore pressure immediately after installation. It is generally accepted (Kirby, Esrig, and Murphy 1983; Randolph, Carter, and Wroth 1979; Wroth, Carter, and Randolph 1979) that soil will return to K_o, conditions for normally consolidated soil, with the radial effective stress equal to the maximum principal stress.

Pile loading

29. Various attempts have been made to determine the effects of pile loading on the state of stress in the soil. Initially, it was assumed that the soil was at the critical state after consolidation so that the mean effective stress would remain constant during shearing (Esrig et al. 1977). Other investigators (Kraft 1982), relying on findings that the soil would not be at the critical state, have used stress paths to predict the state of stress at pile failure. Pile loading effects have also been investigated by using the finite element method with a one- or two-dimensional scheme (Baguelin and Frank 1980; Baguelin, Frank, and Jezequel 1982; Potts and Martins 1982). Pile loading has also been modeled with a three-dimensional finite element program using the state of stress after consolidation as input, but which did not model the effective stress changes during pile loading (Heydinger and O'Neill, in preparation).

Pile capacity predictions

30. Effective stress methods predicting side resistance have been proposed. Esrig and Kirby (1979) developed a set of curves to determine β as a function of the soil OCR and plasticity index. These curves result in

overpredictions of capacity, with β ranging from 0.3 from a normally con-
solidated soil to 2.0 for highly overconsolidated soils.

31. A large research effort funded by a number of organizations has re-
sulted in at least four effective stress methods (Kraft 1982). The four meth-
ods reported by Kraft utilize different approaches to predict capacity. Ac-
cording to the first two methods reported by Kraft (1982), the soil is at the
critical state after installation, but is not for the other two methods. The
ratio of the change in mean effective stress during consolidation to the ex-
cess pore pressure varies from 0.25 to about 0.8, depending on the method.
The first and third method listed by Kraft (1982) assumed that the mean effec-
tive stress remains constant during pile loading. However, it is assumed that
the mean effective stress decreases for the other methods. The comparisons of
predicted and measured capacities, using the four effective stress methods and
the α and λ methods, indicated that the effective stress methods could be
used as accurately as the α and λ methods. An underlying problem with the
effective stress methods is in determining soil parameters that are used to
compute the changes in stress.

32. Two other effective stress methods based on predictions of the
effective radial stress after consolidation have been proposed. Results from
a three-dimensional finite element program indicate that the total radial
stress acting on the pile does not change significantly during pile loading
(Heydinger and O'Neill, in preparation). Therefore, by neglecting the
hydrostatic pore pressure, the effective radial stress after consolidation can
be used for the total radial stress in the following expression:

$$f = \sigma_{rc} \tan \phi_{ss} \tag{19}$$

where ϕ_{ss} is the angle of friction between the pile and the soil. The rec-
ommended equation for side shear for the one method is

$$f = \frac{(1 + \sin \phi'_{cs})}{\sin \phi'_{cs}} s_{u_{cs}} + \frac{\Delta\sigma'_{rc}}{u_e} u_e \tan \phi_{ss} \tag{20}$$

where

ϕ'_{cs} = effective angle of friction for soil at the critical state
(large shearing strains)

$s_{u_{cs}}$ = undrained shear strength for soil at the critical state

20

$(\Delta\sigma'_{rc}/u_e)$ = change in effective radial stress divided by the excess pore pressure, u_e

The equation for u_e is

$$u_e = (p'_o - p'_{cs}) + 2 \left(s_u\right)_{cs} \ln\left(\frac{G}{s_u}\right)^{1/2} \tag{21}$$

where

G = undrained shear modulus

$$p'_{cs} = \left(s_u\right)_{cs} / \sin \phi'_{cs}$$

33. The other method used the results from two consolidation models (Carter, Randolph, and Wroth 1979; Heydinger and O'Neill, in preparation) to obtain the effective radial stress after consolidation. An expression for the stress was obtained from the results of a parametric study.

$$\frac{\sigma'_{rc}}{s_u} = 4.80 - 4.57 \log M \tag{22}$$

where $M = (6 \sin \phi')/(3 - \sin \phi')$. The undrained shear strength should be taken as the in situ value.

34. Estimates of $\beta(= f/\phi'_{vo})$ can be obtained from Equations 20 and 22. A range of values of ϕ'_{cs} , $\left(s_u\right)_{cs}/\sigma'_{vo}$, $(\Delta\sigma_{rc}/u_e)$ and G/s_u were substituted into Equations 20 and 21, resulting in a range of values of β between 0.3 and 0.6. A similar procedure was followed with Equation 22 resulting in a range of values of β between 0.3 and 0.55. It is apparent that the computed capacity can be overestimated unless accurate estimates of the respective parameters are made.

Comparison of Predictions

35. Four instrumented pile-load tests were used to compare predictions for side shear. The four pile-load tests are from insensitive, overconsolidated clay at the University of Houston Central Campus (UHCC) (O'Neill, Hawkins, and Mahar 1981); slightly sensitive, normally consolidated clay in San Francisco Bay Mud (SFBM) (Kirby and Roussel 1979 and 1980); sensitive, lightly overconsolidated clay at St. Alban near Quebec (Bjerrum and Simons

1960; Konrad 1977; Roy et al. 1981); and insensitive, normally consolidated clay at the East Atchafalya Basin Protection Levee (EABPL) (USAE District, New Orleans 1977; Shilstone Testing Laboratory 1976). Measured-side-shear and computed-side-shear distributions are tabulated and ratios of the computed to the measured side shear are given.

36. The side shear was computed at different depths for each of the four tests using five methods. For the α-method, Equation 5 was used as recommended by Dennis and Olson (1983). Side shear was computed for the β-method according to Equation 8, obtained from Meyerhof (1976). Equations 12 and 14 from the statistical studies of Kraft, Focht, and Amarasinghe (1981) were used to compute λ for the λ-method. The other two methods were obtained using Equations 20 and 22. The parameters for Equation 20 were estimated for the St. Alban and EABPL tests since they are not available.

UHCC test

37. The test at the UHCC site was part of a testing program sponsored by the Federal Highway Administration. The stratigraphy for the UHCC test consists of 1.5 ft of clay fill underlain by two formations of clay which were preconsolidated by dessication. The top 4 ft of the lower formation, from a depth of 26 to 30 ft, was appreciably softer than the soils above and below. Undrained shear strengths were obtained from unconsolidated, undrained (UU) and consolidated, isotropic, undrained (CIU) triaxial testing. The test pile and test that was modeled for this research was reference Pile 1 and Test 1, conducted 19 days after pile driving. The test pile was a steel pile, 10.75-in. outside diameter (OD) and 10-in. inside diameter (ID). The pile was driven 43 ft below ground surface and was instrumented with strain gage locations 5 ft apart. The pile was loaded in increments of approximately 10 tons that were maintained for periods of about 1 hr until plunging failure occurred. The measured- and computed-side shear for the test is shown in Table 2.

SFBM test

38. The SFBM test was conducted at Hamilton Air Force Base. The subsurface conditions consist of a single deposit of relatively homogeneous marine clay to a depth of at least 50 ft. It is a very soft clay except for the top 6 ft which is dessicated. The undrained shear strengths were obtained from unconfined compression, UU and field-vane shear tests. The test pile was 4.5-in. OD by 4.0-in. ID sections jacked to a depth of 40 ft. Instrumented with strain gage locations spaced at 5-ft intervals, the pile was loaded to

failure in approximately 10 min by applying 30 small-load increments every 20 sec. The measured and computed side shears are shown in Table 3.

St. Alban test

39. The St. Alban test was conducted near Quebec, Canada. The subsurface consists of a foot of topsoil, 4 ft of weathered clay crust, 27 ft of soft silty clay of marine origin, 13 ft of very soft clayey silt, and a dense layer of sand below a depth of 45 ft. The soil was overconsolidated due to secondary consolidation effects. The undrained shear strengths were obtained from the average of field vane tests which were less than strengths obtained from UU tests. For this report, Pile 6 was used to compute side resistance. The pile was a steel casing with an 8.625-in. OD and a 7.99-in. ID. The pile was jacked to a depth of 25.3 ft below ground surface with an oversized pilot hole 4 ft deep. Loads were measured only at the top and the bottom of the pile, leaving the average side friction for use in the comparisons. Results of a test conducted at 472 hr were used. Load increments of about 139 lb were maintained for periods of about 15 min until failure occurred after 3 hr. The measured and computed side shears are given in Table 4.

EABPL test

40. The load test was on the EABPL, Test I-2. The soil profile consists of 84 ft of soft to stiff clay underlain by 20 ft of silt. Undrained shear strengths were estimated using unconfined compression, UU and CIU tests. A concrete prestressed pile 14 sq in. was used. Instrumented gage locations were placed at 8-ft intervals. The pile was driven and then tested approximately one month after driving. The pile was loaded in increments of 10 tons for periods of about 1 hr except for the 40-ton load which was held for 24 hr. The comparisons of side shear are given in Table 5.

Conclusions and Recommendations

41. Predictions of axial capacity can be obtained most reliably by using total stress methods. The recommendation is to use the lesser of the capacities computed with the α-method by Dennis and Olsen (1983) shown in Figure 5, or the β-method using Equation 8. The predicted side capacity, as it is developed along piles, can vary significantly for the two methods. The computed side shear is greater near the ground surface for the α-method and lesser at greater depths, compared to the β-method. The β-method is

consistent with observations that the unit side shear increases with depth.
The λ-method can result in unconservative values of capacity. The analyses
for the recommended procedures were determined principally from the result of
pile pipes so additional data with concrete piles and H-piles are desirable.

42. Effective stress methods generally result in unconservative predic-
tions of pile capacity. There are too many unknown soil parameters that are
necessary for effective stress methods. Additionally, the methods were devel-
oped for impermeable cylindrical piles and not for concrete or H-piles. Other
effects of driving that the models do not account for are lateral pile wobble
and repeated soil shearing during pile driving.

PART III: PILE SIDE SHEAR-DISPLACEMENT FUNCTION

Introduction

43. Research on pile side shear-displacement functions has occurred as a result of experimental observations that side shear that is mobilized is dependent on vertical pile displacement (Coyle and Reese 1966, D'Appolonia, Poulos, and Ladd 1971) and because of their use in soil-structure interaction programs (Radhakrishnan and Parker 1975). Piles have been instrumented with strain gages at various levels in order to measure the distributions of loads along piles. Load distribution curves were then used to compute mobilized side-shear and vertical pile-displacement relationships. The relationships, f-z curves, are nonlinear functions of side shear and vertical pile displacement. Soil-structure interaction programs are algorithms that model piles as discrete elements. The programs use f-z curves to define the load-transfer behavior at the pile-soil interface in order to determine load-deformation behavior of piles. The purpose of this section is to discuss recommendations for the determining f-z curves.

Methods for Computing f-z Curves

44. Four methods for computing f-z curves were investigated. The computational procedures are presented in this section. The next section consists of an evaluation of the four methods.

Coyle and Reese method

45. Coyle and Reese (1966) used the results of full-scale and laboratory testing in order to develop a procedure for determining f-z curves. The recommendation was to use Figure 9 to determine the effective shear strength and Figure 10 to determine the load transfer, normalized by the effective shear strength, for a number of pile movements. The load transfer is computed by multiplying the effective shear strength by the normalized load transfer for a number of vertical pile movements.

Vijayvergiya method

46. A parabolic expression was proposed by Vijayvergiya (1977b) to compute f-z curves. According to this method, the pile movement should be normalized by the critical pile movement, z_c , that occurs when the maximum side
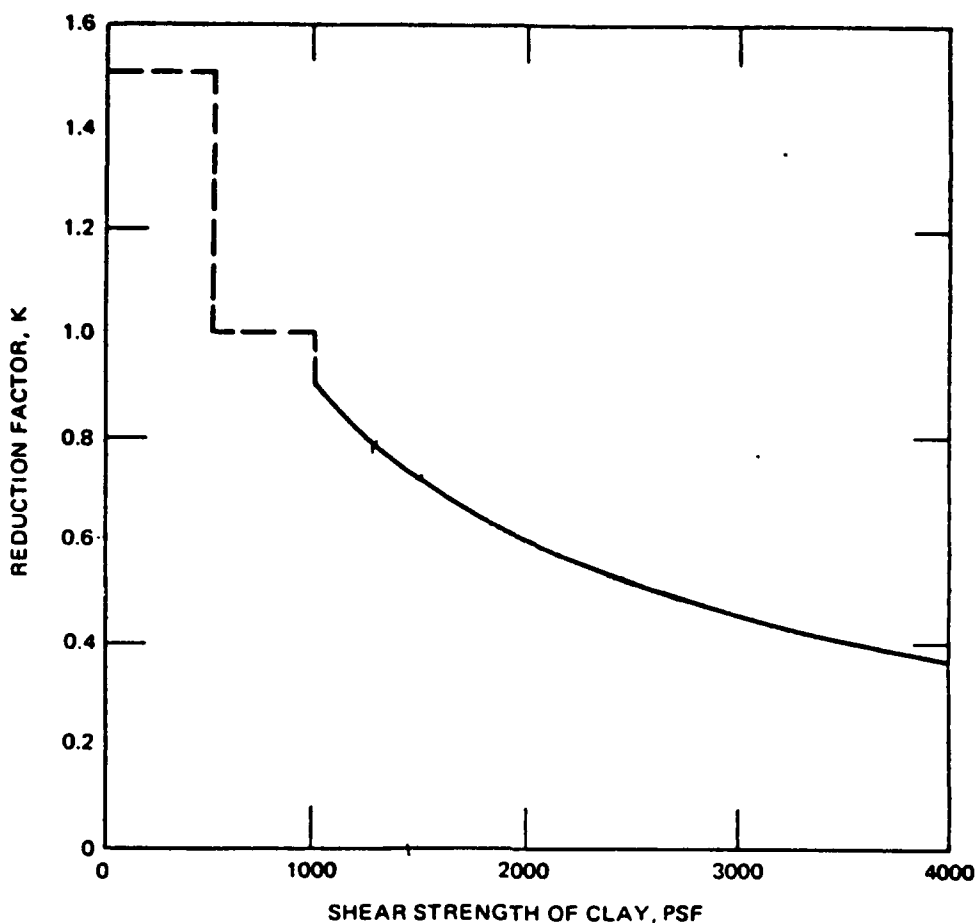
25

Figure 9. Shear strength reduction factor, K
(Radhakrishnan and Parker 1975)

fraction, f_{max} , is mobilized. The equation is

$$f = f_{max} \left(2 \sqrt{\frac{z}{z_c}} - \frac{z}{z_c} \right) \qquad (23)$$

The recommendation was to use z_c equal to 0.25 in. f_{max} is the side shear capacity which, for practical purposes, can be determined by any method.

Kraft, Ray, and Kagawa method

47. The method proposed by Kraft, Ray, and Kagawa (1981) is a modification of an approximate elastic solution proposed by Randolph and Wroth (1978). According to the method, the vertical displacements at a given level along the pile are approximated by a curved surface, with displacements decreasing as the radial distance from the center of the pile increases. The curved surface is approximated with concentric cylinders of shear. It is assumed that the radial displacements are negligible compared to the vertical displacement,

26
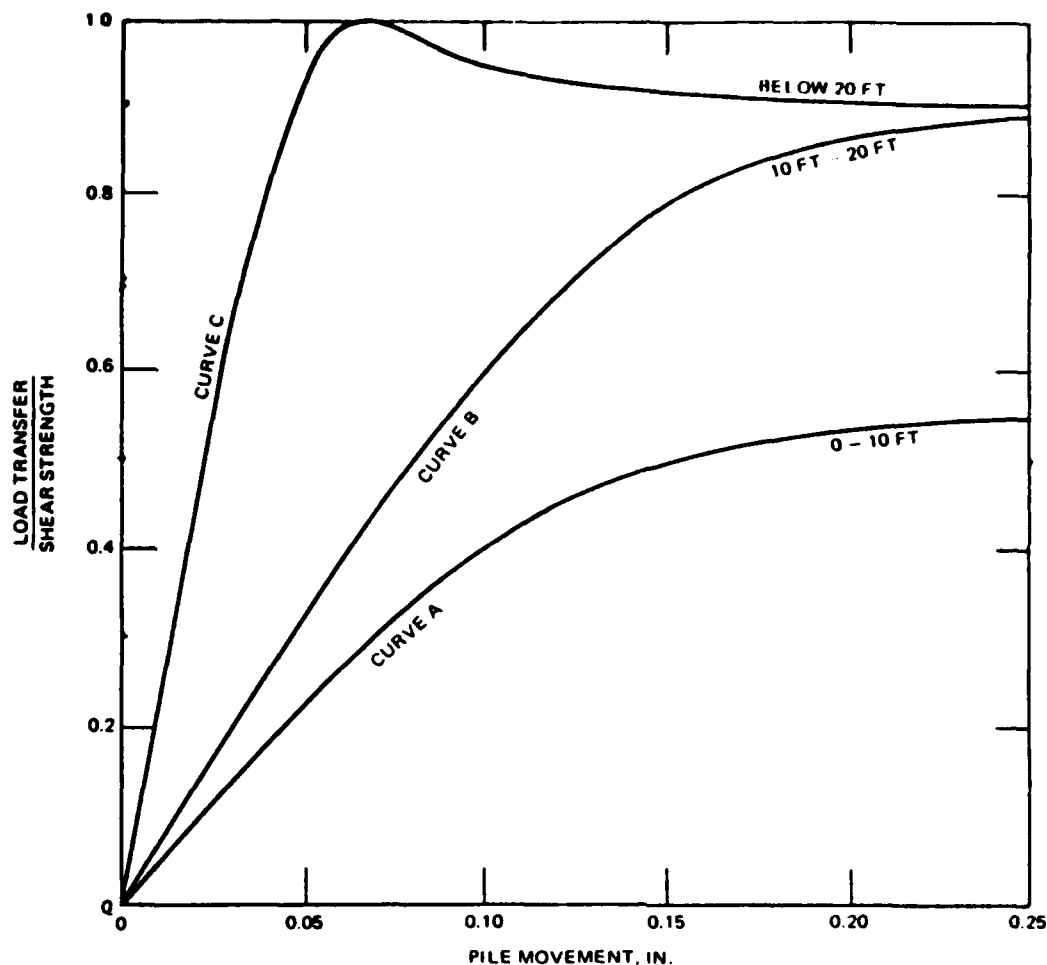
Figure 10. Normalized load transfer versus vertical pile
movement (Radhakrishnan and Parker 1975)

which then results in simple shear conditions. For simple shear, the product
of the shear stress, τ , at radial distance, r , from the pile center and the
radial distance is constant. It is assumed that the shear stresses are negli-
gible at a radial distance, r_m , where the boundary of the zone of influence
is given in Equation 24,

$$r_m = 2.5 \ L\rho \ (1 - \nu) \tag{24}$$

where

   L = pile length

   ν = Poisson's ratio of the soil

   ρ = ratio of the shear modulus at depth L/2 to the shear modulus at
        the pile tip.

27

48. The load-displacement relationship is obtained by integrating the shear strains from the pile surface, r_o, to the boundary of the zone of the influence. Since the product r times τ is constant, Equation 25 is obtained for the relationship,

$$z_s = \tau_o r_o \int_{r_o}^{r_m} \frac{dr}{Gr} \qquad (25)$$

where

z_s = vertical displacement at the pile surface

τ_o = soil shear stress at the pile surface

G = soil shear modulus

Because of the effects of pile installation and soil consolidation, the shear modulus increases approximately linearly with radial distance from the pile until the undrained modulus is reached at a radius of r_m. It was shown by Kraft, Ray, and Kagawa (1981) that the average shear modulus after soil consolidation does not vary significantly from the initial shear modulus for undisturbed soil, G_i, for soil at very low strains. Therefore, the radial variation of the shear modulus due to pile installation was neglected and the variation of the shear modulus due to shear stress was considered.

49. A secant modulus formulation was used to approximate the variation of the shear modulus with shear stress. The variation is expressed by the following hyperbolic equation

$$G_o = G_i \left(1 - \frac{\tau_o R_f}{\tau_{max}} \right) \qquad (26)$$

where

R_f = stress-strain curve-fitting constant

τ_{max} = maximum shear stress that is mobilized at pile failure

No specific recommendations were given for estimating R_f when shear stress-strain data are not available. It is typically in the range of 0.9 to 1.0.

50. An expression for the vertical pile displacement is obtained by substituting Equation 26 for Equation 25. The resulting expression is

$$z_s = \frac{\tau_o r_o}{G_i} \ln \left(- \frac{\frac{r_m}{r_o} - \psi}{1 - \psi} \right) \qquad (27)$$

28

where

$$\psi = \frac{\tau R_f}{\tau_{max}} \tag{28}$$

Equation 27 can be solved for a number of vertical pile displacements by selecting different values of shear stress that are less than the maximum shear stress. The resulting data can be plotted as a curve of shear stress versus vertical pile movement, which would be the desired f-z curve.

Heydinger and O'Neill method

51. A general equation for side shear as a function of pile movement normalized by pile diameter, z/D, was proposed by Heydinger and O'Neill (in preparation). The equation for side shear is

$$f = \frac{E_{fz} \frac{z}{D}}{\left(1 + \left|\frac{E_{fz} \frac{z}{D}}{f_{max}}\right|^m\right)^{1/m}} \tag{29}$$

where

E_{fz} = slope of the initial tangent to a curve of f versus z/D

m = shape parameter

For the investigation, three well-instrumented pile-load tests were modeled extensively using an approximate solution to determine the effects of pile installation and a finite element formulation on model pile loading. A parametric study was conducted with the finite element program in order to determine the effects of pile properties on the shapes of f-z curves. The computed f-z curves were optimized for the parameters in terms of soil and pile properties.

52. Expressions for the parameters E_{fz} and m were obtained as follows. E_{fz} is given as the ratio of the initial undrained soil modulus, E_u, and a parameter K. An expression for K was determined as a function of the pile length to diameter ratio, L/D as shown in Figure 11. The expression is

$$K = \exp\left(0.36 + 0.38 \ln \frac{L}{D}\right) \tag{30}$$

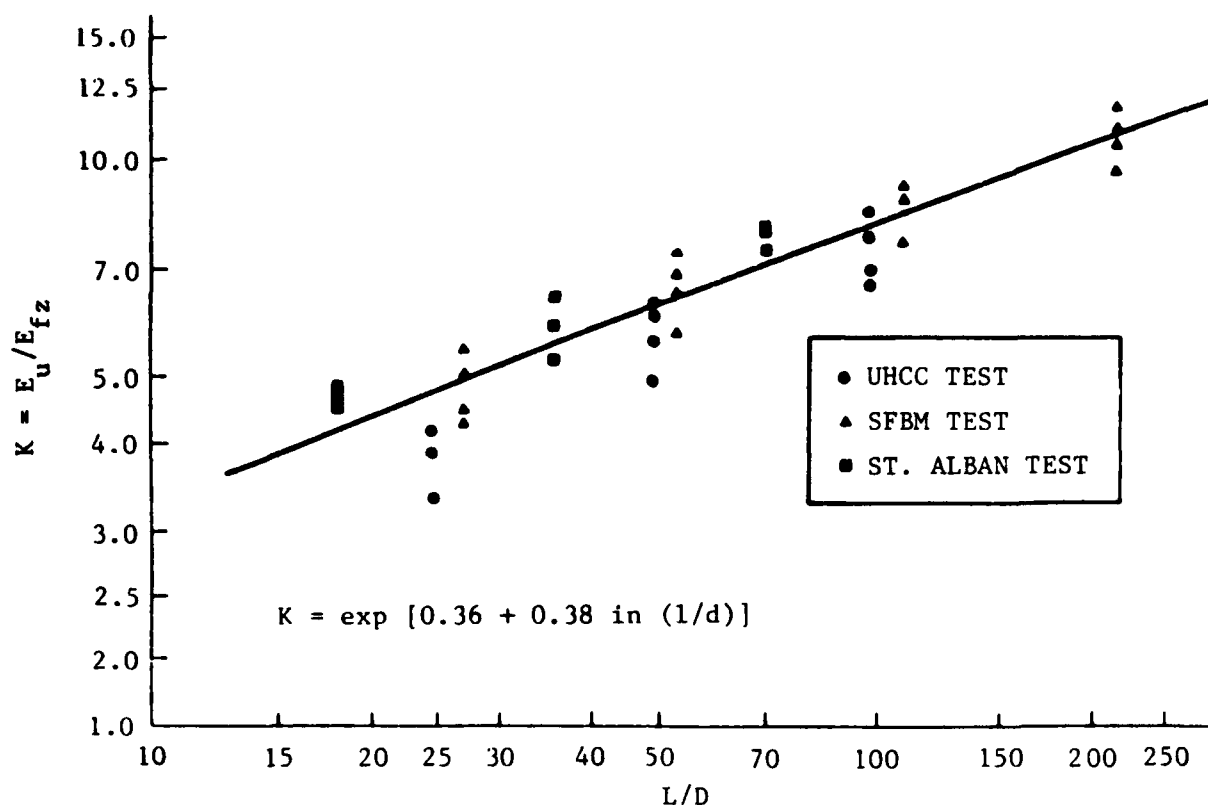The shape parameter was plotted as a function of the pile L/D ratios as

29

Figure 11. ln K versus ln (L/D)

shown in Figure 12. The intercept values for m , referred to as m_o , were plotted as a function of the ratio $\left(E_u\right)_{ave}/P_a$ as shown in Figure 13, where $\left(E_u\right)_{ave}$ is the average undrained soil modulus for a soil stratum and P_a is atmospheric pressure. A linear regression analysis was used to obtain Equation 31 for the shape parameter.

$$m = \exp\left\{0.12 + 0.54 \ln\left[\frac{\left(E_u\right)_{ave}}{P_a}\right] - 0.42 \ln \frac{L}{D}\right\} \qquad (31)$$

The reason that the pile movements were normalized by the pile diameters and $\left(E_u\right)_{ave}$ was normalized by atmospheric pressure was to nondimensionalize the parameters.
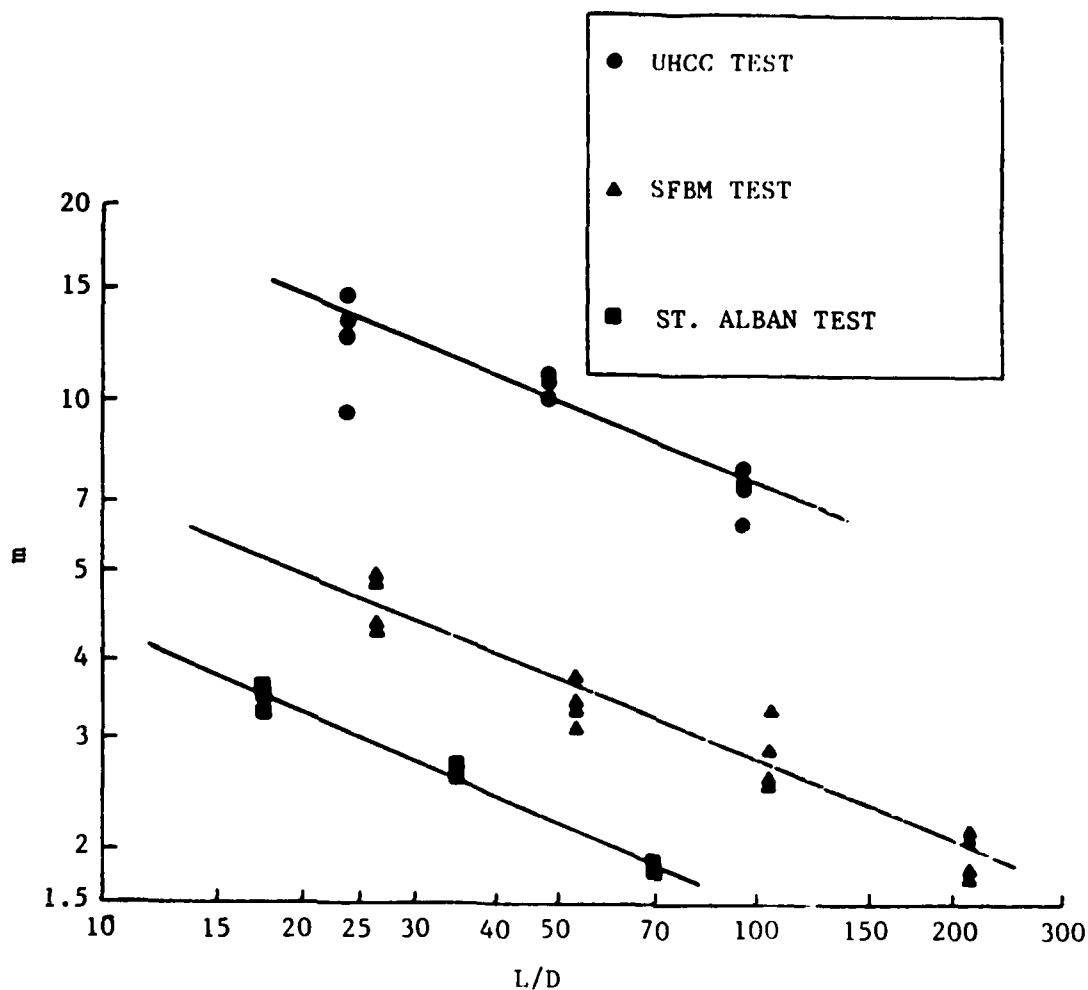
Figure 12. ln m versus ln (L/D)

Example of Predictive Methods

53. The following computational results illustrate the use of the four predictive methods. For this example, a pile with an outside diameter of 1 ft and a length of 75 ft was modeled. The f-z data was computed for a depth of 22.5 ft.

54. Soil properties representative of a normally consolidated soil were used for the computations. A wet unit weight of 112.4 pcf and a depth to the water table of 15 ft were selected. The mean effective overburden pressure was computed assuming k_o equal to 0.58. An undrained shear strength of 721 psf was computed using the ratio s_u/σ'_{vo} equal to 0.35 ($s_u/p'_o = 0.49$) . The maximum side shear was computed using the α-method as recommended by
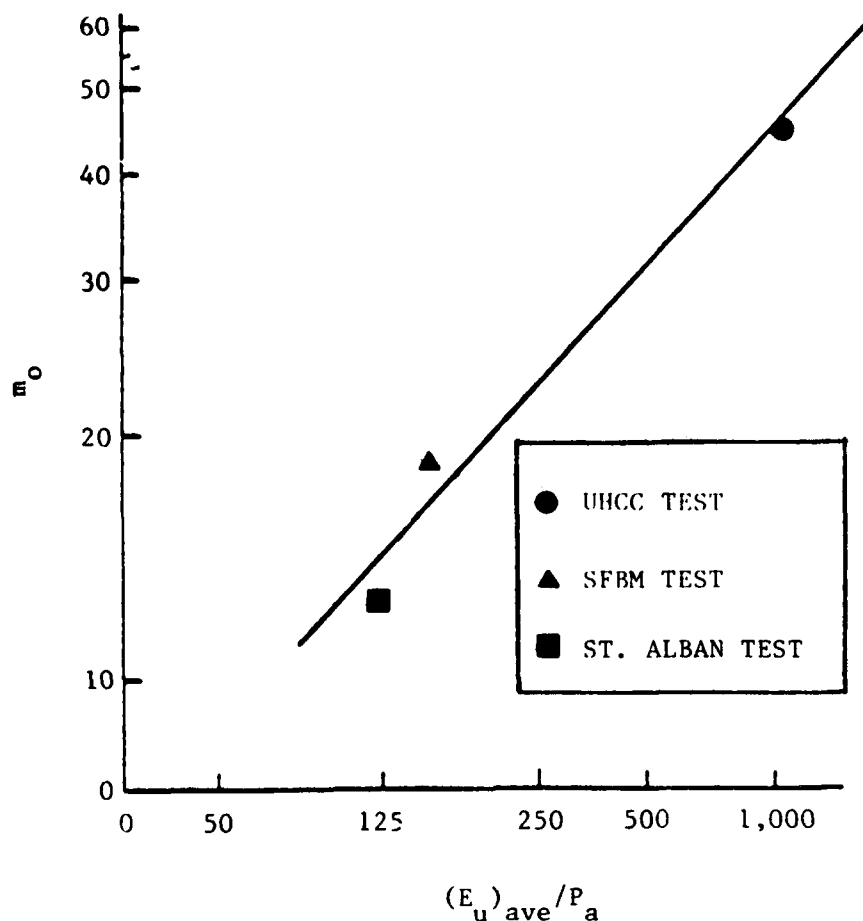
31

Figure 13. ln m_o versus $\ln\left(E_u\right)_{ave}/P_a$

Dennis and Olson (1983). Thus $\alpha = 0.90$ and $f_{max} = 648$ psf were obtained. The undrained soil modulus, equal to 865,800 psf, was computed using the ratio E_u/s_u equal to 1,200. The undrained shear modulus, G , is one third of E_u .

55. Data for the computed f-z curves are given in Table 6. The assumed pile movements in the first column were used for the first three methods shown. To compute values of side shear for the method by Coyle and Reese (1966) values of the ratio of the load transfer to the shear strength, obtained by using "Curve C" in Figure 10, were multiplied by 648. Equation 23 was used with $f_{max} = 648$ and $z = 0.25$ in. to compute values of side shear for the Vijayvergiya (1977b) method. For the Kraft, Ray, and Kawaga (1981) method, values of pile movement were computed using Equation 27 for selected values of side shear ranging from 0.10 times f_{max} to 0.95 times f_{max} . The

32

zone of influence, r_m , was computed using $\nu = 0.5$ and $\rho = 0.616$. The parameter ψ was computed assuming $R_f = 1$. For the method by Heydinger and O'Neill (in preparation), values of $K = 7.395$ and $m = 5.672$ were determined using Equations 30 and 31, respectively, with $L/D = 75$. An average value of $E_u = 1,212,000$ psf was computed for the soil along the total length of embedment. Computed values of side shear were determined for the assumed pile movements using $E_{fz} = E_u/k = 117,086$, $D = 12$ in. and $f_{max} = 648$.

Discussion of Predictive Methods

56. The method by which the four predictive methods are compared by evaluating them according to their ability to account for different factors that affect the shapes of f-z curves. Factors affecting f-z curves are concerned with pile and soil properties. The pile properties that have been considered are length, diameter, L/D ratio, and stiffness. For the purpose of the discussion on pile properties, it has been assumed that the magnitude of f_{max} would not be affected by pile properties as reported from theoretical analyses (Heydinger and O'Neill, in preparation). Soil properties include undrained shear strength, stiffness, depth, sensitivity, and stress history.

Pile length

57. The effects of pile length have been investigated. Elasticity (Randolph and Wroth 1978) or finite element (Heydinger and O'Neill, in preparation) solutions indicate that soil shears caused by pile loading encompass larger areas radially for longer piles. The integral equation of the displacement in the shear zones, Equation 25, indicates that displacements for a given level of side shear would be greater for longer piles. This implies that f-z curves would be less linear and that displacements required to mobilize maximum side shear would be greater for longer piles.

58. Predicted f-z curves would be affected with two of the four methods. According to the Kraft, Ray, and Kawaga (1981) method r_m would be greater for longer piles. Therefore, predicted values of pile movement using Equation 27 would be greater for longer piles. With side shear plotted as the ordinate and pile movement as the abscissa, f-z curves would be shifted towards the right as pile length increased. With the method by Heydinger and O'Neill (in preparation), the parameter K increases as the length or L/D increases as in Equation 30; therefore, the initial slope of the f-z curves,

33

$E_{fz} = E_u/K$, decreases. The parameter m , Equation 31, decreases as L increases also, and the f-z curves shift to the right as m decreases. Both of these parameters would then result in a shift to right of the f-z curve as pile length increases.

Pile diameter

59. Pile diameter affects the shape of f-z curves and the movement, z_c , required to mobilize f_{max} . The radial zone around piles where soil is remolded during installation and sheared during pile loading increases as pile diameter increases. Consequently, larger vertical pile displacements are required to mobilize side shear for larger diameter piles. These findings have been verified by elasticity solutions and finite element analyses. Figure 14 shows the results of finite element analyses (Heydinger and O'Neill, in preparation) where diameters were varied. By increasing diameters (decreasing L/D ratios), the f versus z/D curves shifted to the left. If plots of f
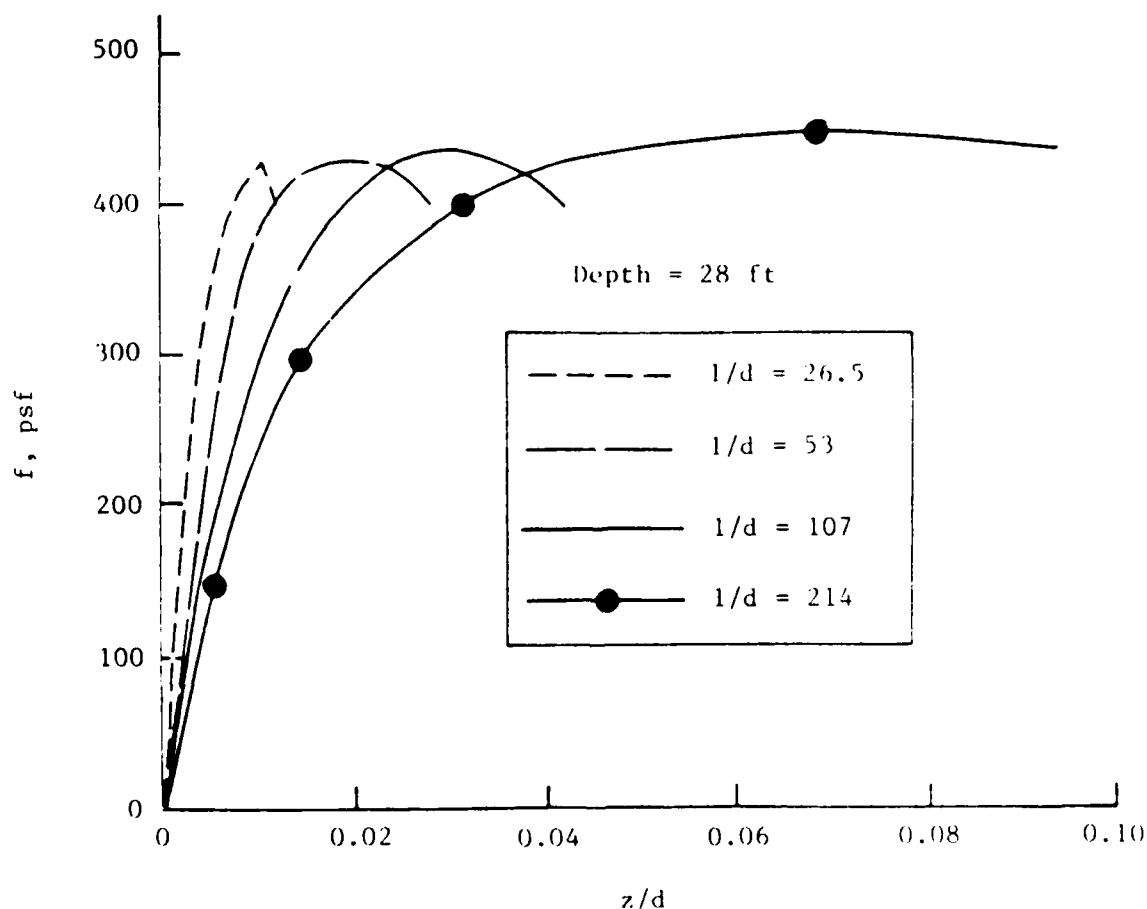

Figure 14. Side resistance versus z/D ratio from
Finite Element Method parametric study, SFBM test

34

versus z were made for the curves, the initial slopes of the curves would be greater for the larger values of L/D . Thus, there is no unique curve for f versus z/D or for f versus z .

60. Three of the methods can account for the effect of diameter. The method by Vijayvergiya (1977b), Equation 23, would result in a shift of f-z curves to the right if it were assumed that z_c increased with diameter. For the Kraft, Ray, and Kawaga (1981) method, with Equation 24, the term with r_m/r_o tends to cause z_s to decrease as the diameter increases, but the overall effect is for z_s to increase as diameter increases since z_s is directly proportional to r_o . According to the method by Heydinger and O'Neill (in preparation), K , Equation 30, decreases as L/D decreases and E_{fz} = E_u/K increases. The shape parameter, Equation 30, increases as L/D decreases. Thus, E_{fz} increases and m increases as diameter increases (L/D decreases), but the computed side shear decreases since E_{fz} is multiplied by z/D in Equation 29. The effect of increasing the diameter then is to shift f-z curves to the right. Figure 15 indicates the variation of the computed f-z curves.

L/D ratio

61. An additional verification to the effects of pile length and diameter on the initial slopes of f-z curves is obtained in terms of the L/D ratio from the work of others. Theoretical results by Baguelin and Frank (1980) were reported giving the slope of the initial tangent to the f versus z/r_o curves as a function of the ratio G_i/k , where G_i is the initial shear modulus. The parameter k is shown in Figure 16 as a function of L/D . The figure illustrates that the slope increases as L/D increases. Equivalent results were also plotted for K using Equation 28 and assuming that E = 3G . Figure 16 indicates that there is close agreement between results obtained from the theoretical studies and those that are obtained from the method by Heydinger and O'Neill. Similar results could be obtained using the method by Kraft, Ray, and Kawaga (1981).

Pile stiffness

62. Pile stiffness, usually expressed as the product of the cross-sectional area and Young s modulus of the pile, has been investigated (Heydinger and O'Neill, in preparation). Values of the stiffness were varied by factors of 10 and 1/10 for the finite element analyses of three well-instrumented pile-load tests. By comparison of the predicted f-z curves,

35
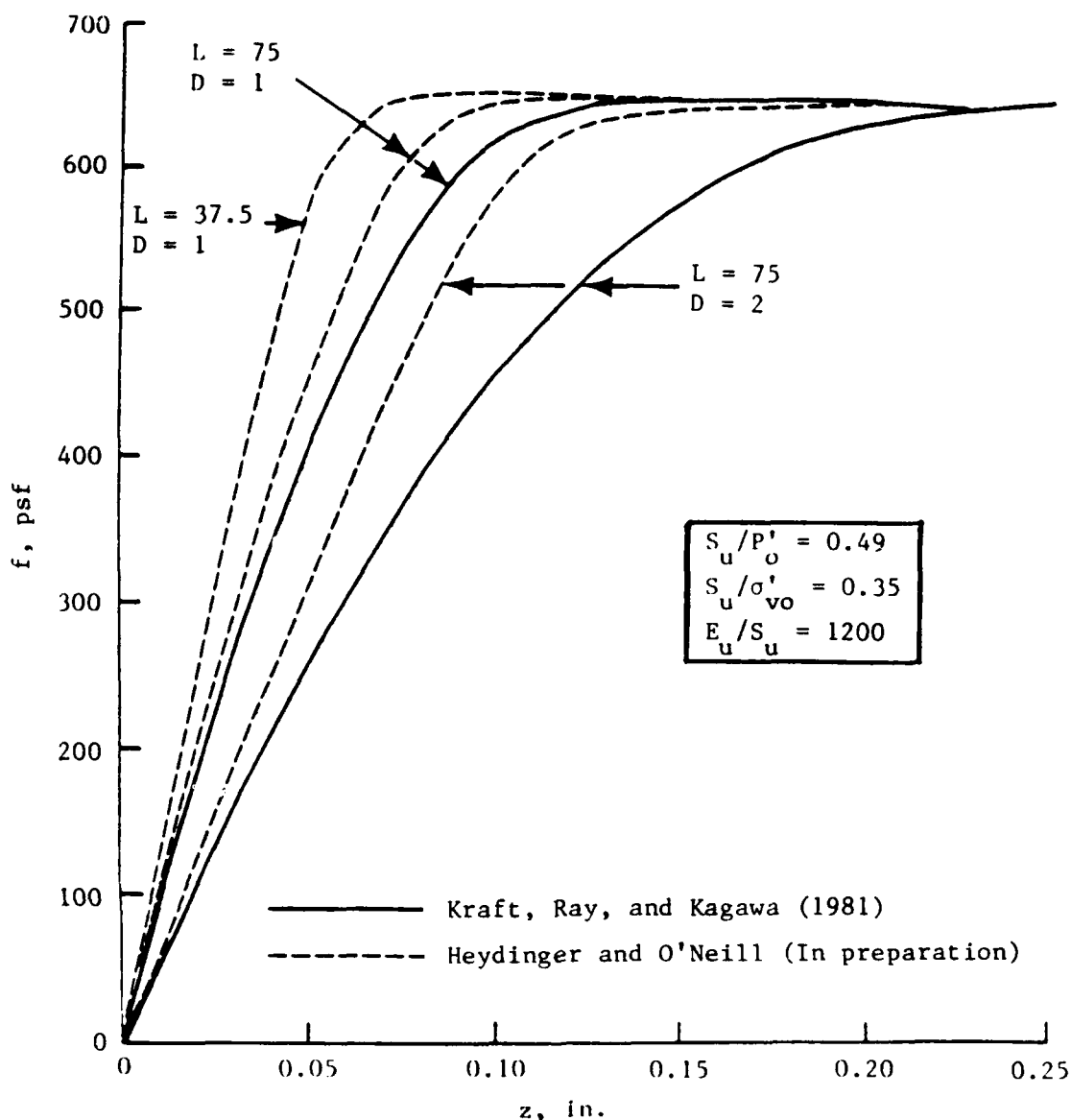
Figure 15. Effect of pile length and diameter on f-z curves

it was determined that pile stiffness does not nfluence the shapes of f-z curves significantly. However, the load-deformation behavior of the pile top is affected by its stiffness since the compressibility changes. The predictive methods consequently do not include pile stiffness as a variable.

Undrained shear strength

63. For the purpose of this comparison, the undrained shear strength or f_{max} is considered since f_{max} is dependent on this strength. The Coyle and Reese (1966) procedure utilizes curves of mobilized side resistance divided by the effective undrained shear strength which is equivalent to f_{max}. The

Figure 16.   Initial slope of f-z curves
(Heydinger and O'Neill, in preparation)
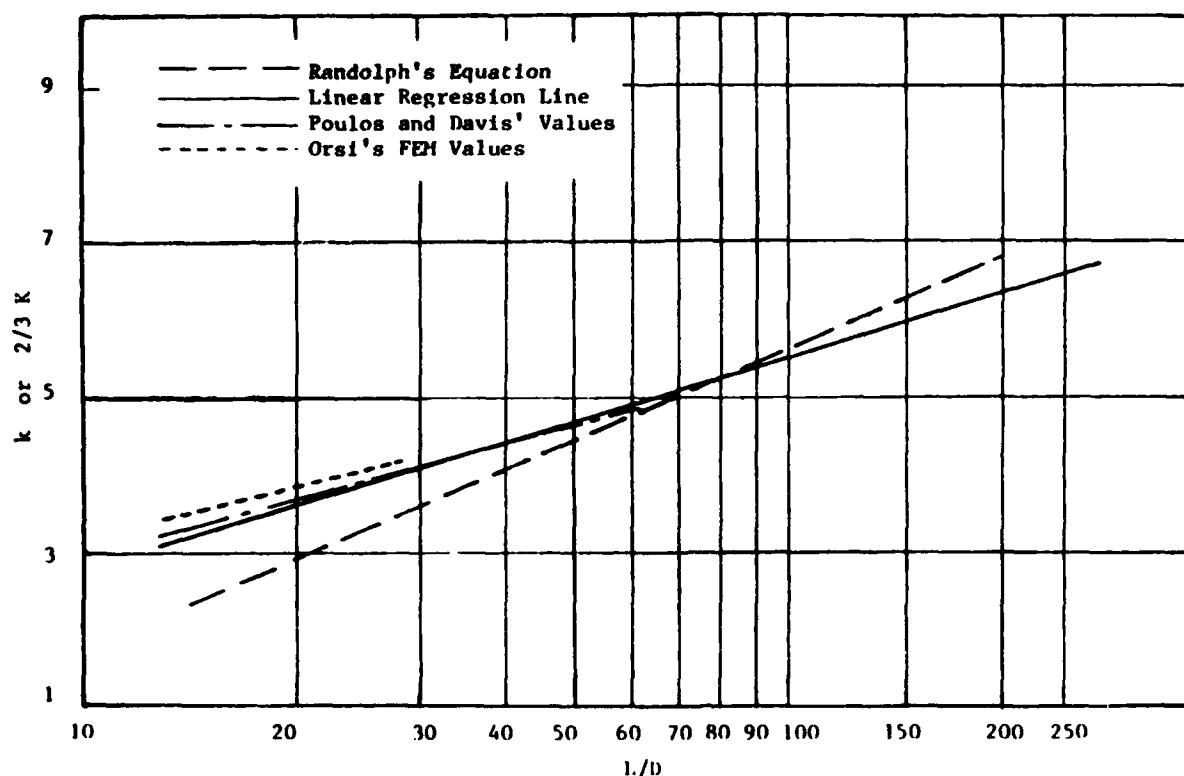
undrained shear strength was determined from unconfined compression tests. The
basis for the three recommended curves is the trends that were observed from
field and laboratory tests. Vijayvergiya (1977b) proposed a parabolic equa-
tion for f/f_{max} as a function of z/z_c using the curves recommended by
Coyle and Reese (1966). However, efforts to normalize f-z curves using
f/f_{max} did not result in strong trends for the initial slopes or the shapes
of the f-z curves as a function of depth or soil stiffness for the three
pile-load tests reported by Heydinger and O'Neill (in preparation). In any
case, computed values of mobilized side resistance are directly proportional
to f_{max} for the methods by Coyle and Reese (1966) and Vijayvergiya (1977b).

64.   The other two methods rely on the stress level to determine the de-
gree of nonlinearity of the f-z curves. The stress level is expressed as
the ratio f/f_{max} . For the Kraft, Ray, and Kawaga (1981) procedure, the pa-
rameter ψ which is proportional to the stress level, occurs in Equation 27.
For the method by Heydinger and O'Neill (in preparation), the term E_{fz}

37

$(z/D)/f_{max}$ in the denominator of Equation 29 is equivalent to the stress level. For both methods the stress level influences the curvature of f-z curves. Computed values of z or f are not directly proportional to estimated values of undrained shear strength or f_{max} , so the procedures are not as sensitive to errors in estimating the quantities.

Soil stiffness

65. Soil stiffness can be expressed in terms of Young's modulus or shear modulus. In this case, undrained moduli were used to represent undrained pile loading. Methods that include a soil modulus correlate the interaction behavior at the pile-soil interface to the soil stiffness. There is a rational basis for such procedures since the side shear-deformation behavior of soil near the pile surface is related to the stress-strain properties of soil.

66. Two methods rely on soil moduli to compute f-z curves. The Kraft, Ray, and Kawaga (1981) solution incorporates a hyperbolic expression to represent the average shear modulus, which is dependent on the level of stress. Since z is inversely proportional to the initial shear modulus in Equation 27, error involved in estimating G_o is directly evident throughout the computations. The general equation, Equation 29, has both theoretical and empirical basis for computing f-z curves as a function of E_u . With this method, errors in estimating E_u result in errors for E_{fz} and the shape parameter m . However, the error diminishes as the stress level increases. Figure 17 illustrates the effects of varying soil stiffness for the two methods.

Soil depth

67. Soil depth affects soil confining pressures. Coyle and Reese (1966) showed that load transfer increased with depth. They attributed the effect of depth to the fact that there are vibrations during driving which open small spaces between the pile and the soil which may not close near the ground surface after driving. Therefore, three curves were recommended depending on depth.

68. According to theoretical approaches, side shear is dependent on soil shear strength and confinement, and side shear-deformation behavior is dependent on the soil stiffness. When using Equation 27, the computed pile movements decrease when f_{max} or the soil modulus increase. Similarly, the computed mobilized side shear increases when f_{max} or the soil modulus in Equation 29 is increased. Thus, assuming one or both of the factors increase

38
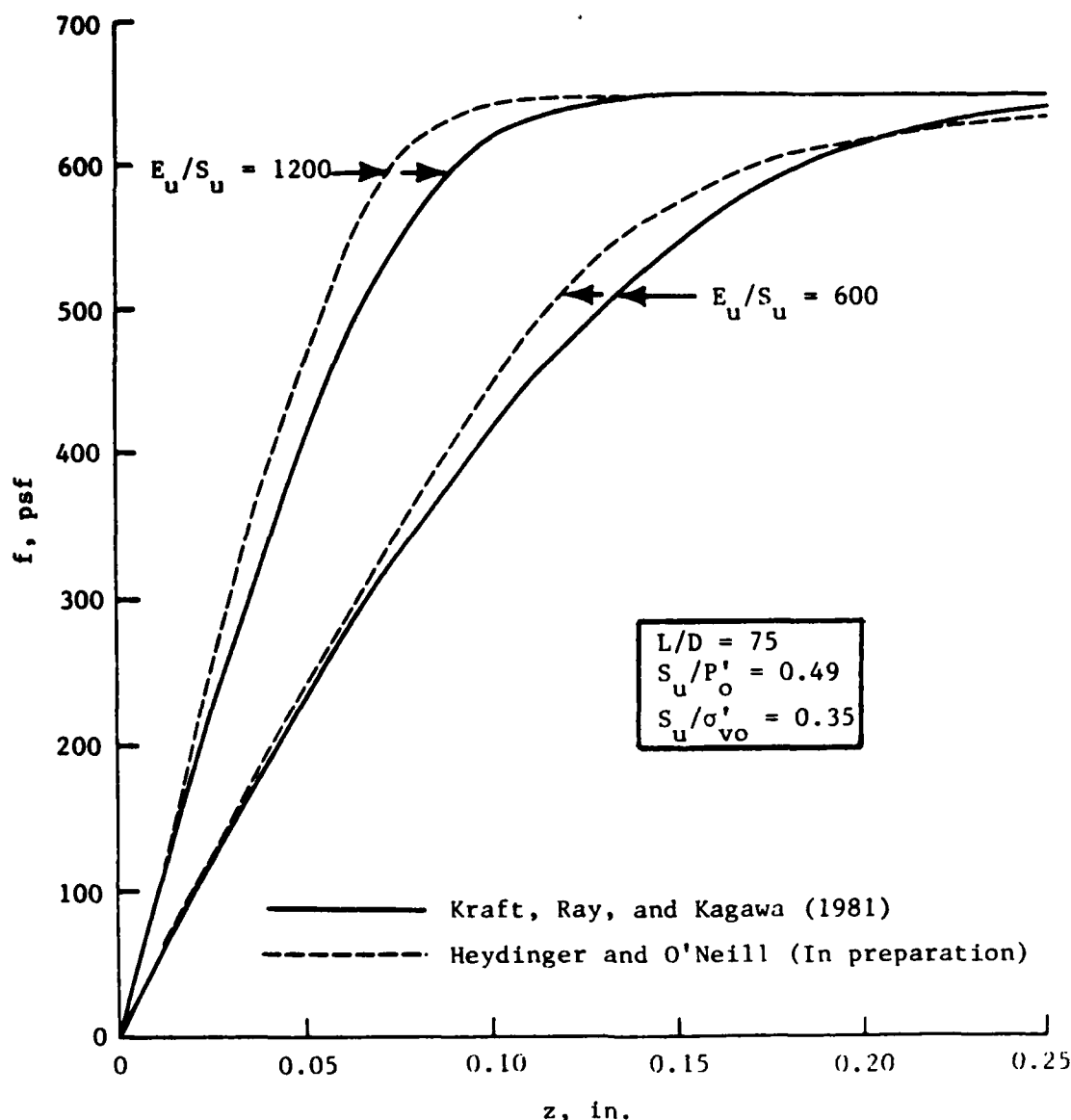
Figure 17. Effect of soil stiffness on f-z curves

with depth, the f-z curves would shift upward as could be expected. The methods cannot account for spaces between pile and soil if they exist. Side shear should be ignored where the spaces exist.

69. The measured results from three pile-load tests were used to develop the parameters for the general equation. Typically the f-z curves were shifted upward with increases in depth. However, when attempting to correlate K and m with depth, it was determined that no definite correlation between the parameters could be made with depth. Therefore, the same values of K and M should be used for a given pile unless, for the case of m,

there are strata with significant differences in the undrained soil modulus.

Soil sensitivity and remolding

70. Soil sensitivity affects the properties of soils when they are remolded during pile installation. It has been reported (Coyle and Reese 1966) that soft, insensitive clays can have higher undrained shear strengths after the soil reconsolidates around piles. On the other hand, triaxial testing on sensitive clays (Roy et al. 1981) have shown that the strengths and moduli of remolded clays were reduced by 30 and 65 percent, respectively, due to remolding. However, it has not been shown conclusively that soil properties after reconsolidation would be significantly reduced.

Stress history

71. Stress history is represented by the overconsolidation ratio. Overconsolidation can occur as the result of glaciation, sediment erosion, dessication, and because of secondary consolidation effects. Profiles of normally consolidated soils consist of soils with relatively homogeneous soil properties with depth or gradually changing with depth. Profiles of these soils generally exhibit a marked decrease in overconsolidation effects with depth. Methods by Coyle and Reese (1966) and Vijayvergiya (1977b) relying principally on s_u or f_{max} to compute f-z curves do not account for overconsolidation effects adequately. The other two methods make use of soil moduli which account for overconsolidation effects. Figures 18 and 19 illustrate predicted f-z curves by the four methods for normally consolidated and overconsolidated clays, respectively. The data listed in Table 6 were used to plot the curves in Figure 18.

Comparison of Predictive Methods

72. The four instrumented pile-load tests that were used to evaluate the proposed methods for predicting side shear were also used for comparing f-z curves. Representative f-z curves were selected for each of the four tests. Soil properties were estimated from the reports of the pile-load tests. For the first three tests, the soil properties were those interpreted for the finite element analyses that were used to develop the general equation (Heydinger and O'Neill, in preparation). The α-method recommended by Dennis and Olson (1983) was used to compute f_{max} for the comparisons.

40
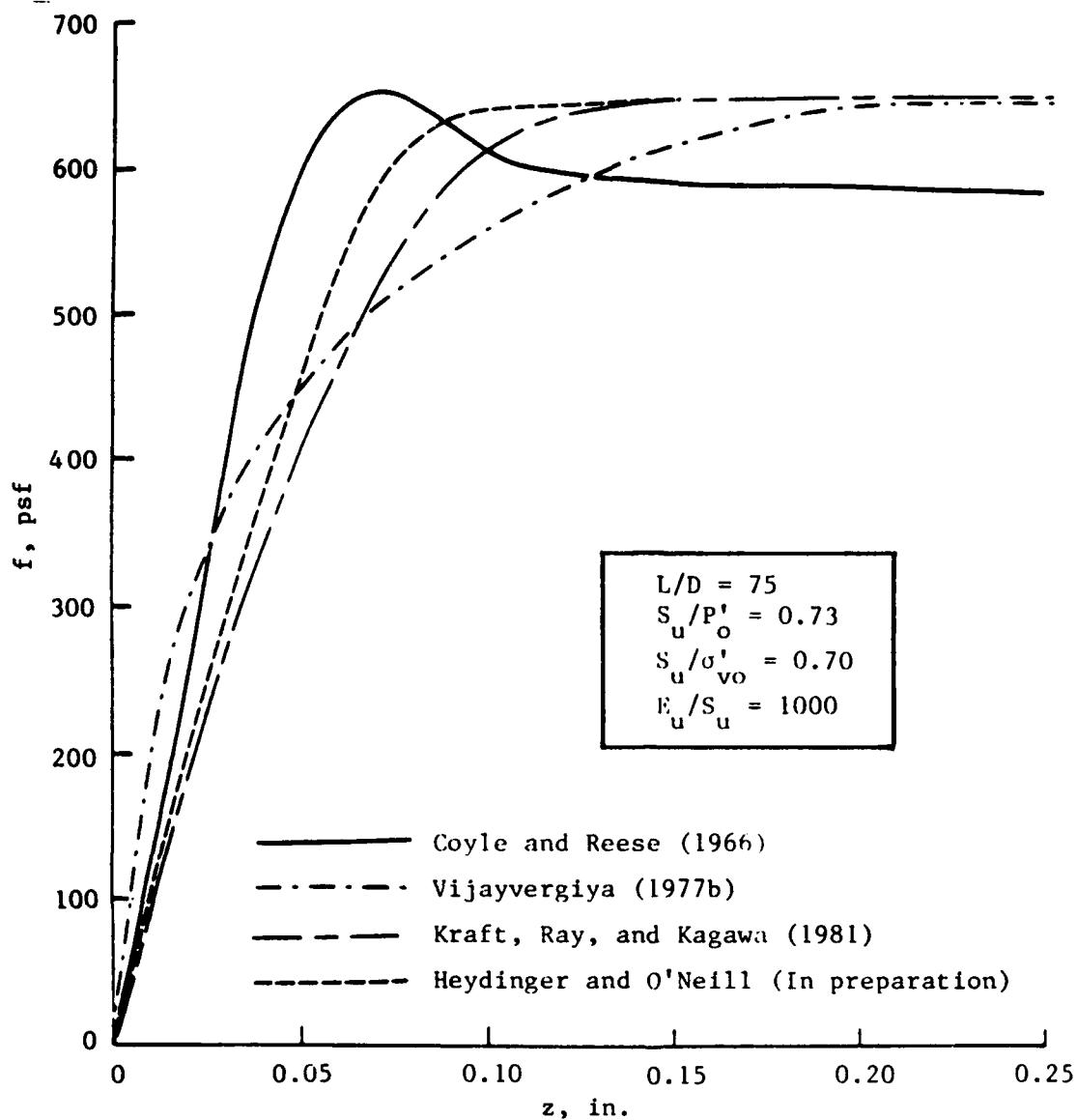
Figure 18. Predicted f-z curves for normally consolidated clay

UHCC test (O'Neill,
Hawkins, and Mahar 1981)

73. Computed f-z curves were obtained for two depths, 21 and 36 ft.
Values of E_u corresponding to values of E_u/s_u equal to 1,000 and 900, re-
spectively, for the two depths. The values of E_u are higher than values in-
terpreted from triaxial or pressuremeter tests and are lower than values in-
terpreted from crosshole shear tests. The computed results were compared to
measured results at nearby depths. The comparisons are shown in Figure 20.
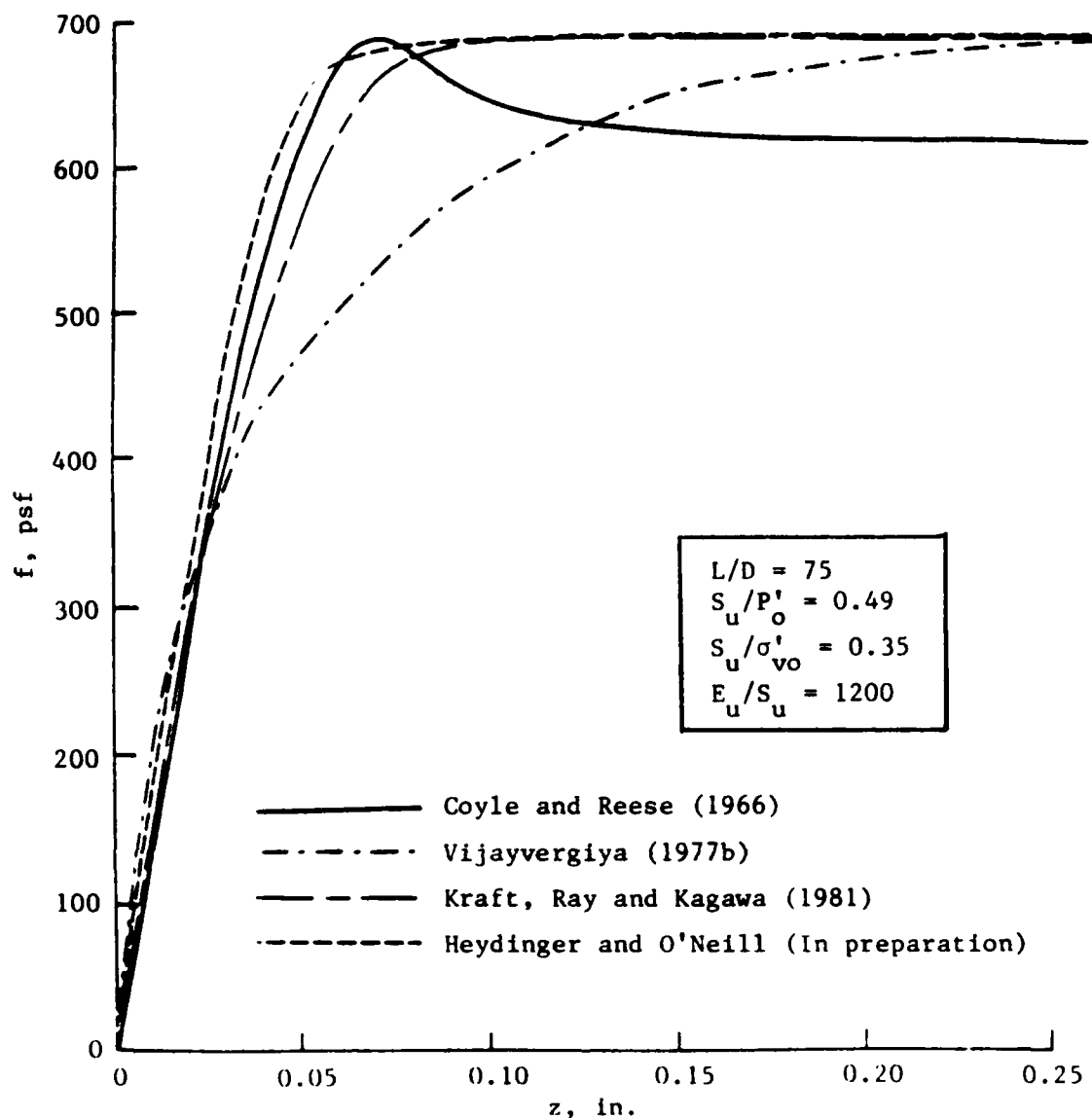
Figure 19. Predicted f-z curves for overconsolidated clay

SFBM test (Kirby and
Roussel 1979 and 1980)

74. The computed and measured results are for depths of 20 and 35 ft. Values of E_u/s_u equal to 600 were used to estimate E_u, as recommended by Kirby and Roussel (1979 and 1980). They are representative of moduli obtained from triaxial tests at low strains. The comparisons are given in Figure 21.
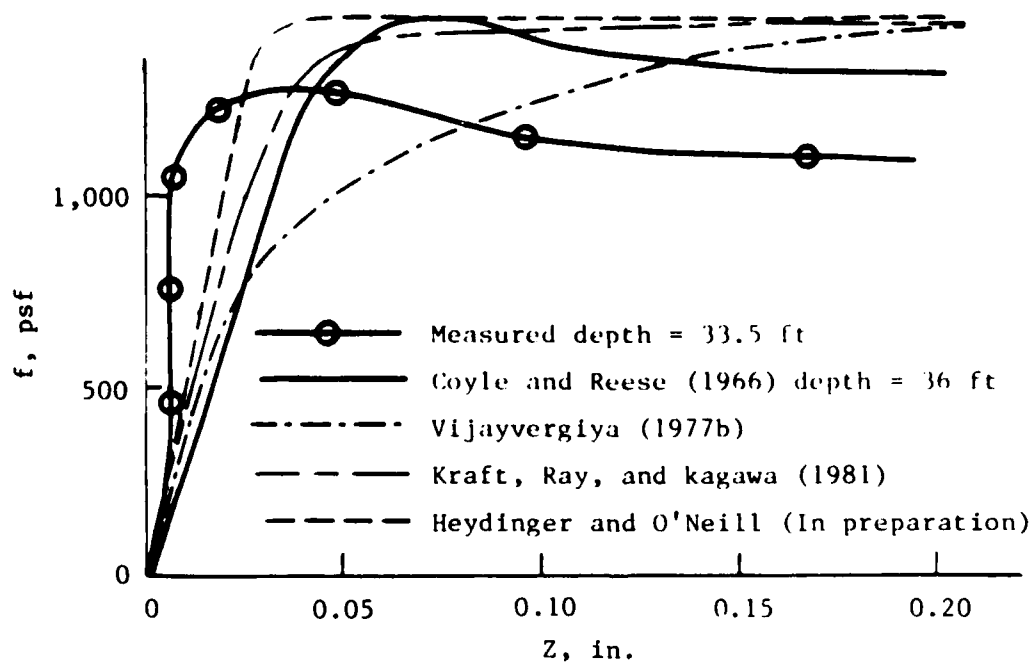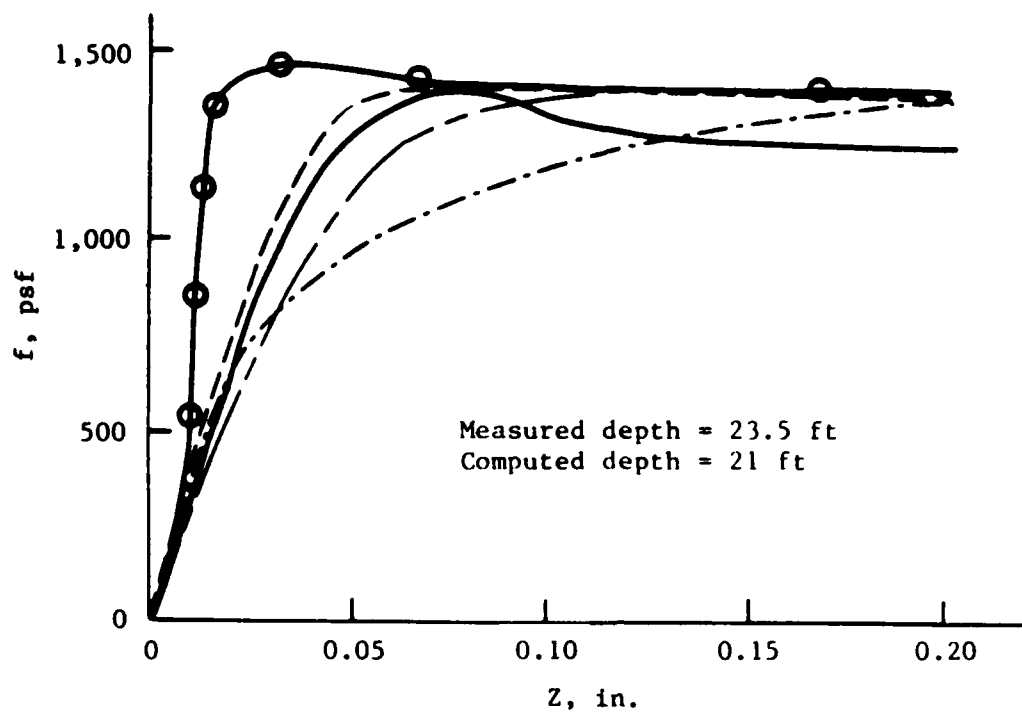
Figure 20. Measured and computed f-z curves for UHCC test

Figure 21. Measured and computed f-z curves for SFBM test

St. Alban test (Blanchet,
Tavenas, and Garneau 1980;
Konrad 1977; Roy et al. 1981)

75. Computed f-z curves were compared to a curve computed from the average measured side friction since strain-gage measurements were not made. A ratio of E_u/s_u equal to 450 was used as recommended (Roy et al. 1981) for remolded soil on triaxial testing. Values of E_u/s_u equal to 900 were obtained from undisturbed or aged samples. The curves are given in Figure 22.
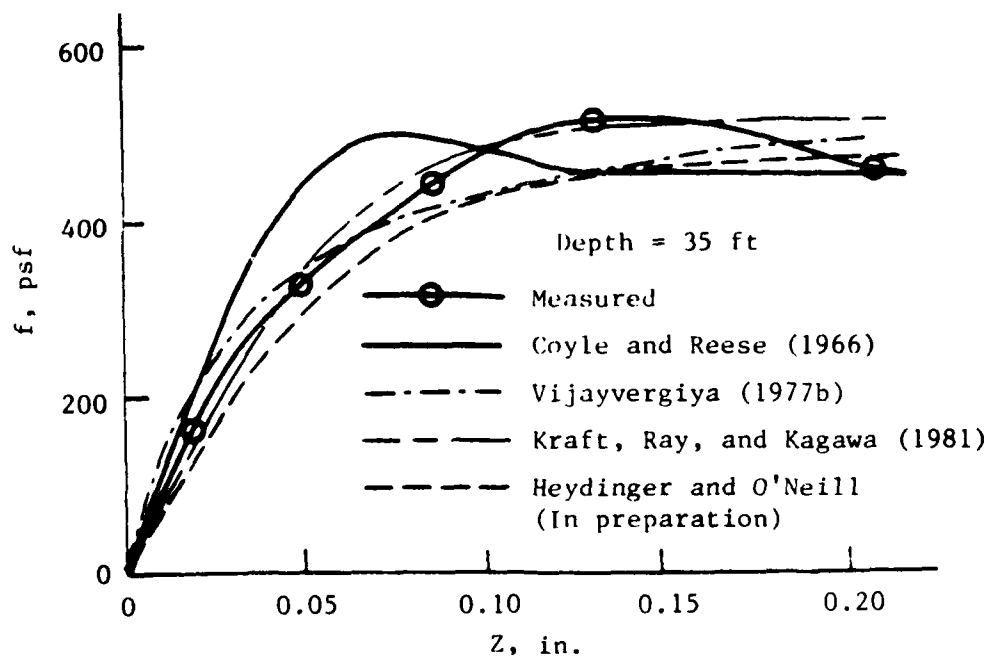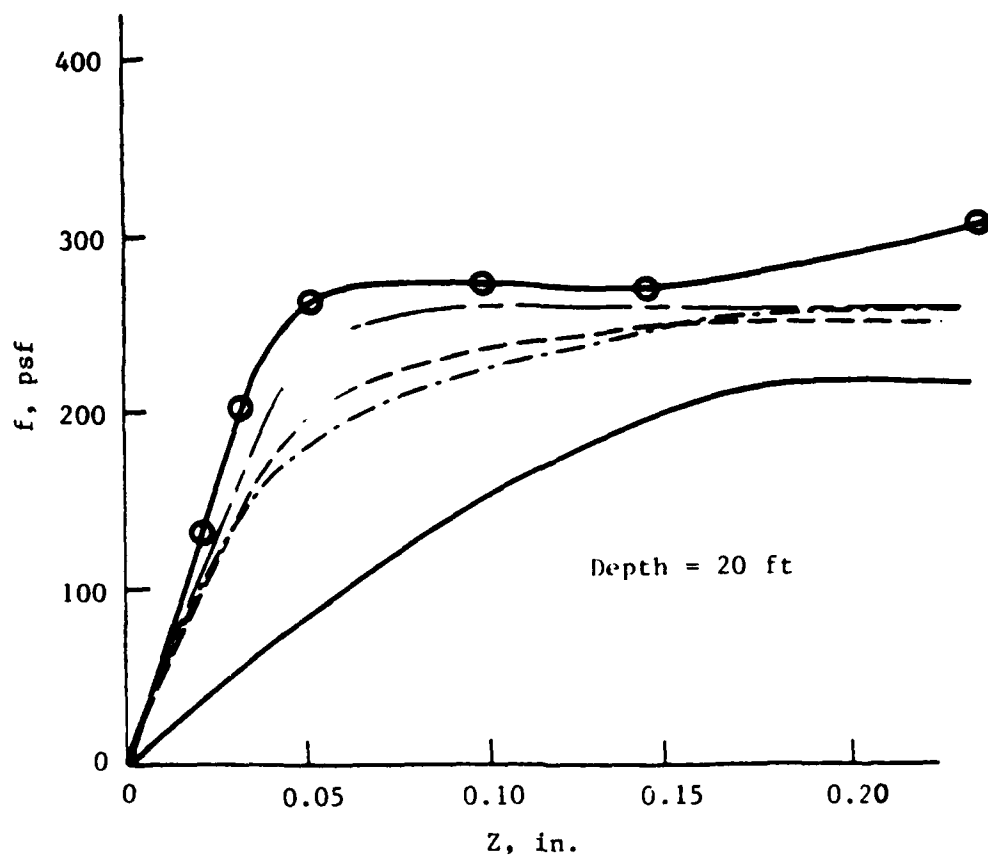
EABPL test (US Army Engineer
District, New Orleans 1977;
Shilstone Testing Laboratory 1976)

76. Computed and measured f-z curves were obtained for depths of 17 and 49 ft. E_u was estimated using E_u/s_u equal to 600. A wide range of values of the ratio E_u/s_u was obtained from triaxial testing, thereby requiring a reasonable estimate. The comparisons are shown in Figure 23.

Soil-Structure Interaction Program

77. The purpose of this section is to illustrate the effects that the shapes of f-z curves have on the predicted load-displacement behavior of the pile top. Of particular interest, were the effects of using nonlinear f-z curves of varying degrees of nonlinearity. This aspect was investigated for soils with properties representative of soft and stiff clays. The effects of varying the initial slopes of f-z curves were also investigated to illustrate the sensitivity of pile-top behavior on the initial slope. The results indicate the importance of accurate determination of f-z curves.

78. For this investigation, the axially loaded pile analyses were conducted using the program titled PX4C3 (Radhakrishnan and Parker 1975), which was developed at the University of Texas at Austin. The program requires input for the pile tip load-deformation behavior, referred to as the Q-z curve, and for a number of f-z curves. In order to investigate the effects of the f-z curve input, Q-z curve data were input and then the f-z curves were varied. The criteria used to determine the Q-z data were given in the documentation for the program (Radhakrishnan and Parker 1975) for the program for soils with no available stress-strain curve. A 50-ft-long pile with an outside diameter of 1 ft and stiffness $AE = 4.37 \times 10^8$ was used
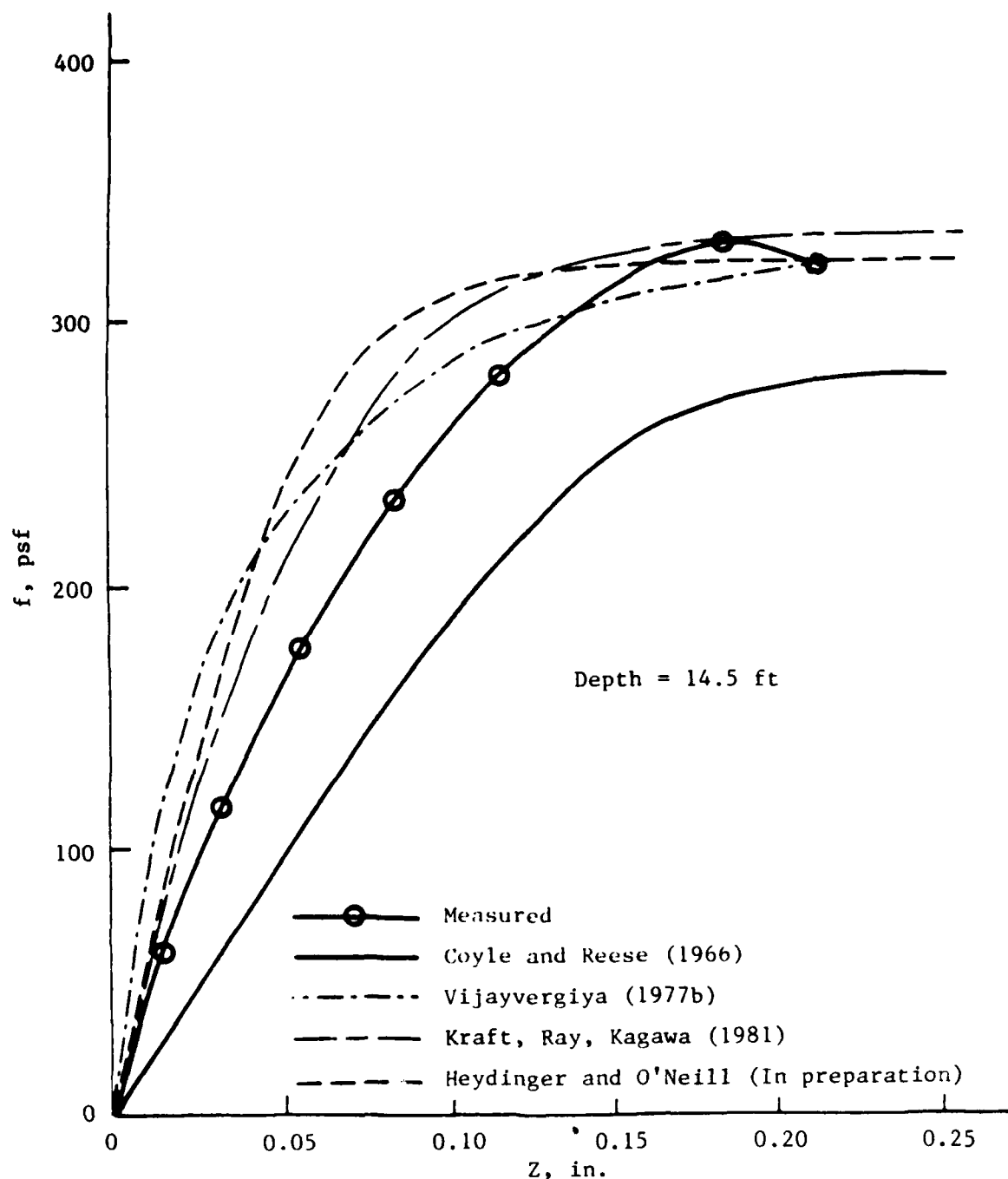
Figure 22. Measured and computed f-z curves
for St. Alban test

throughout. f-z curves were computed for five depths at 10-ft intervals be-
ginning at a depth of 5 ft.

79. The variation of the f-z curves was achieved using the criteria
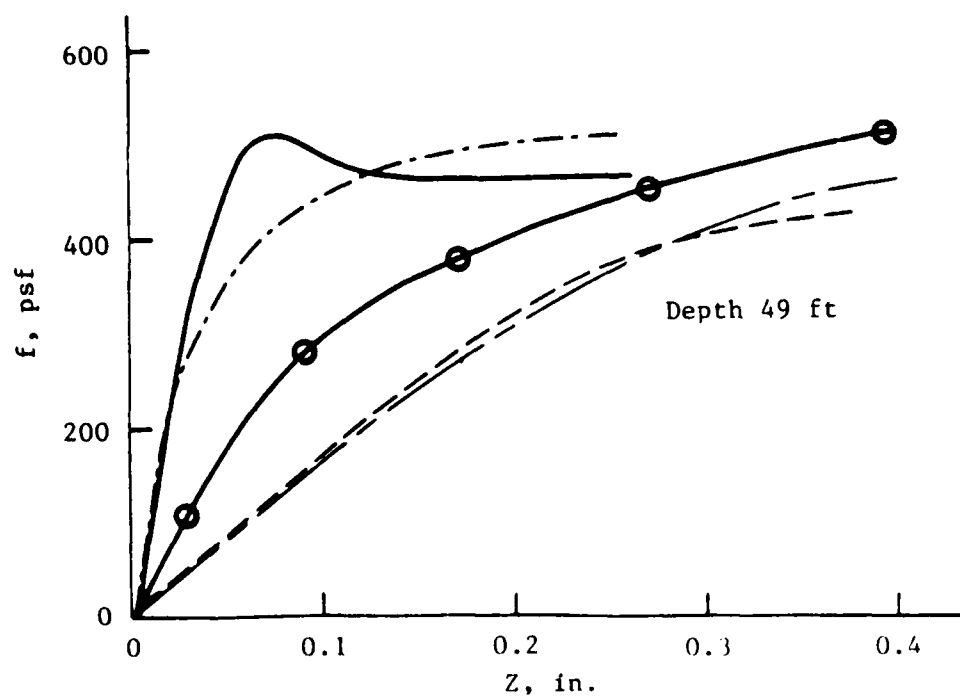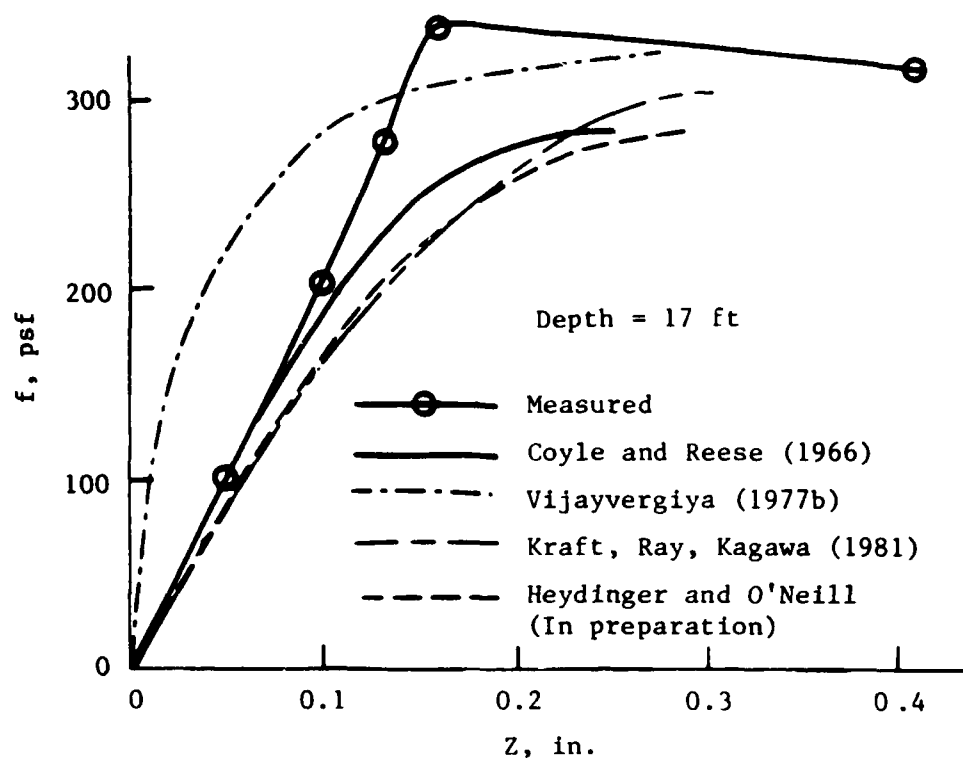by Heydinger and O'Neill (in preparation). With this method, the single

Figure 23. Measured and computed f-z curves for EABPL test

parameter m can be used conveniently to vary the shapes of the f-z curves, and the parameter E_{fz} can be used to vary the initial slope. Similar results can be obtained by varying the parameters for the method by Kraft, Ray, and Kawaga (1981).

Case 1--variation of
f-z curve shapes, soft soils

80. The behavior of a pile in a soft soil was modeled using representative soil parameters for a saturated clay. A saturated unit weight of 102.4 pcf was used to compute the effective vertical overburden pressure distribution. The undrained shear strength was computed at various depths using the ratio of the undrained shear strength to the effective vertical overburden pressure equal to 0.35. The undrained soil modulus was computed using the ratio E_u/s_u equal to 800 and two types of soil profiles were investigated for this case. Profile 1 consists of a soil formation with soil strengths and moduli increasing with depth as determined by the input parameters described above. Profile 2 consists of a single, homogeneous layer of soil having the parameters determined for a depth of 25 ft for Profile 1.

81. The input data for the Q-z curve for Profile 1 was obtained by using the computed soil modulus for a depth of 50 ft. For this case then, E_u = 560,000 psf was computed. The corresponding stress-strain curve and the Q-z data were computed using the recommended criteria (Radhakrishnan and Parker 1975). The same Q-z data were used for Profile 2.

82. Side shear-displacement curves were input for the five depths indicated previously for Profiles 1 and 2. According to Equation 30, the parameter K is 6.34 for L/D = 50 for all depths of Profiles 1 and 2. The initial slope of the line that is tangent to the curve of f versus z was computed using E_u/k . Thus, for example, the average undrained soil modulus at the 25-ft depth, E_u = 280,000 , was used to compute the initial slope to the f-z curves, E_{fz} = 44,164 . The shape parameter, m = 3.14 , was computed using Equation 31 and the average value of E_u . The f-z curves were computed using $f_{max} = s_u$ in Equation 29. Figure 24 shows the computed f-z curves for different values for m for a depth of 25 ft. It indicates the variation of the curves with m and the curve with m = 10 approaches a bilinear curve. Similar sets of curves were obtained for the other depths.

83. The results of the axially loaded pile analyses are shown in Figure 25. For the analyses, sets of f-z curves were input for each of the

48
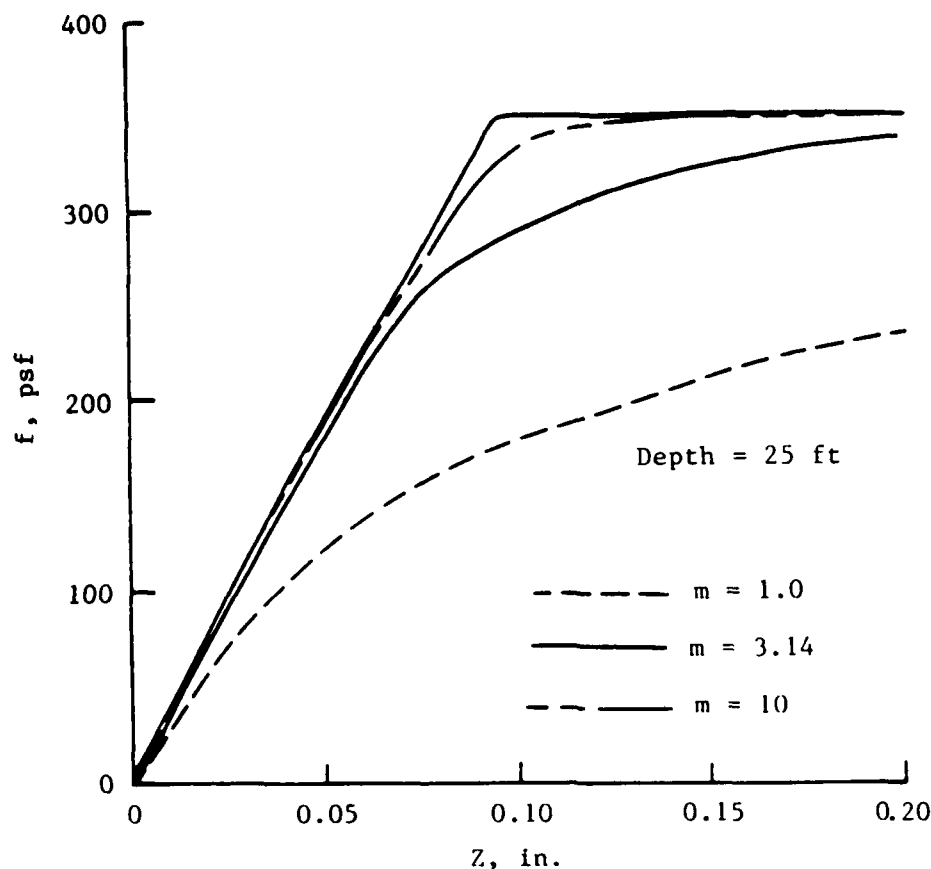
Figure 24. Variation of f-z curves with m

values of m shown in Figure 24. The pile head deformation variation for Profile 1 was 0.15, 0.08, 0.07 in. for m = 1.0 , 3.14, and 10, respectively, for the working loads which were taken as one half the ultimate loads. Also, shown in Figure 25 is the variation of the pile head deformations for Profile 2. The deformations at the working loads are 0.10, 0.07, and 0.06.

Case 2--variation of
f-z curve shapes, stiff soil

84. A homogeneous soil profile was used for the stiff soil analyses similar to the method that was used for Profile 2 for the soft soil analyses. A saturated unit weight of 122.4 pcf was used to compute the vertical effective overburden pressure for a depth of 25 ft, equal to 1,500 psf. The ratio of the undrained shear strength to the effective vertical pressure equal to 0.8 was used to compute s_u = 1,200 psf. An undrained soil modulus, E_u = 1,440,000 psf, was computed using E_u/s_u = 1,200 .

85. The data for the Q-z and f-z curves were computed as described

49

Pile head load, lb
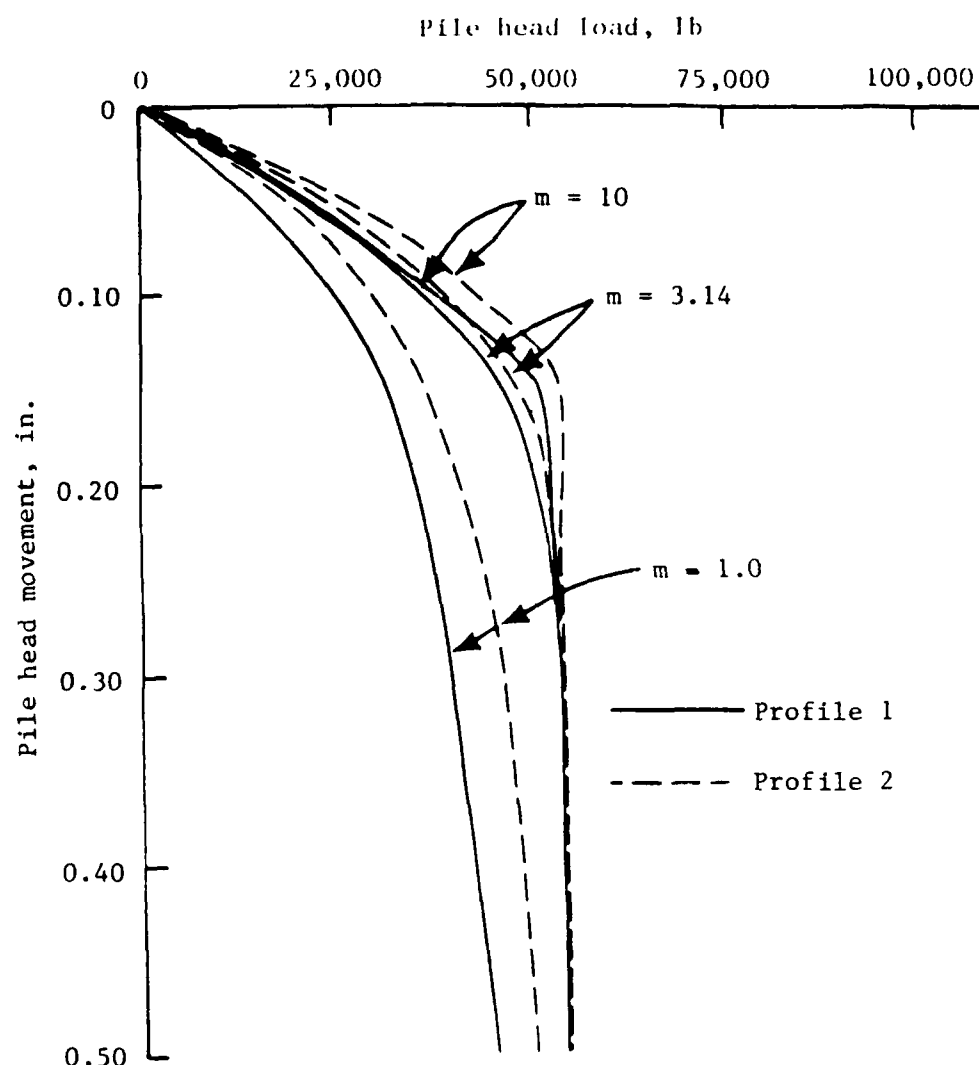
Figure 25. Pile top load versus pile top
movement, Case 1, Profiles 1 and 2

previously. The stress-strain curve was computed by using the undrained soil
modulus. The parameter K = 6.34 remains unchanged. The initial slope is
$E_{fz} = E_u/K = 227,129$. The computed shape parameter is 7.61. The side shear-
displacement curves were computed using $f_{max} = 0.8$, $s_u = 960$.

86. Figure 26 shows the results of the pile analyses for f-z curves
with m = 7.61 and for bilinear functions. The pile head deformation varied
from 0.07 in. for the m = 7.61 to 0.06 in. for the bilinear function for the
working load.

Case 3--variation of ini-
tial slope of f-z curve

87. The analyses with the variation of the initial slopes of the f-z
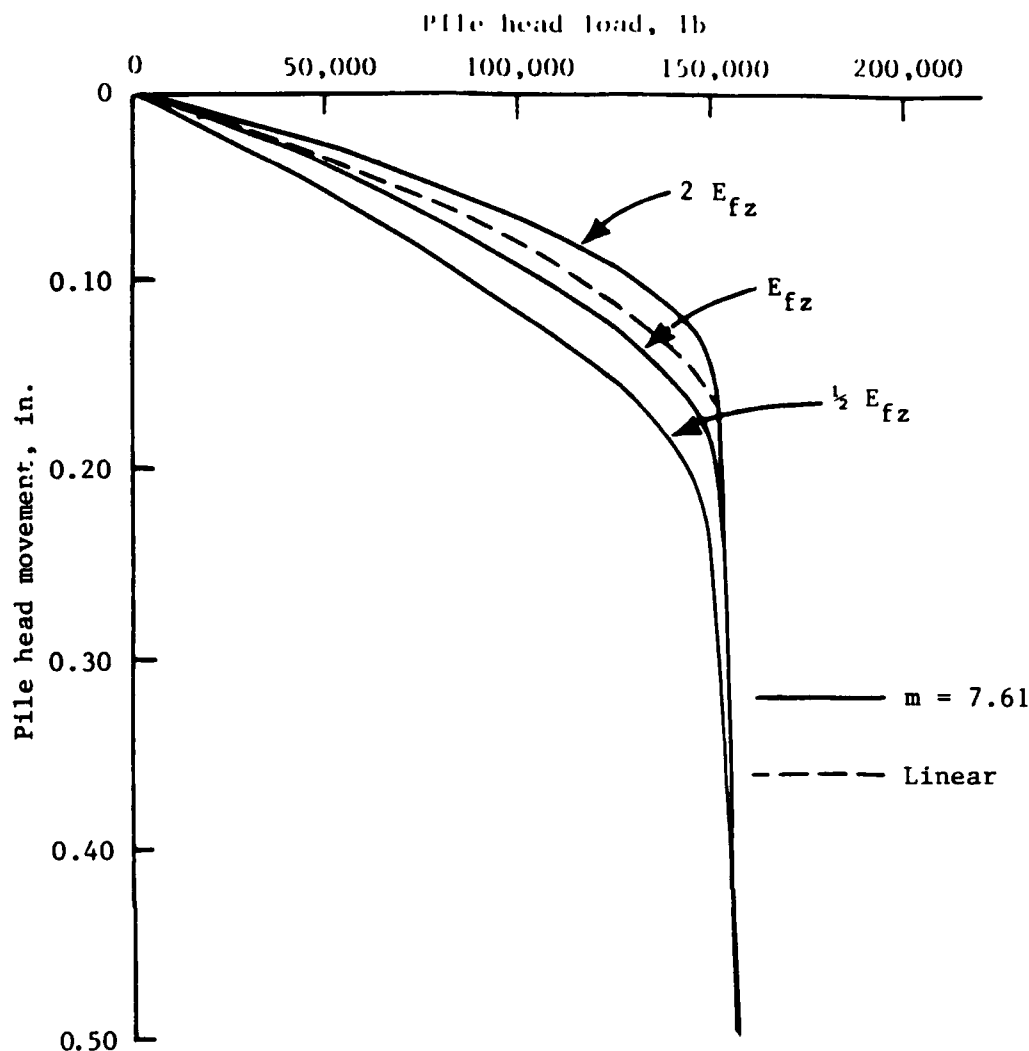
Figure 26. Pile top load versus pile
top movement, Cases 1 and 2

curves, E_{fz} , were conducted for the previous analyses of Case 2 by using m
= 7.61 . The initial slopes were varied by factors of 0.5 and 2 and the re-
sulting f-z curves were input. The results of the analyses are shown in
Figure 26. The pile-top deformation for $2E_{fz}$ is 0.05 in. and the defor-
mation for $(1/2)E_{fz}$ is 0.09 in. The differences in the pile deformations at
the design load would have been larger had bilinear curves been used. For
these three cases, the magnitude of the variations of the pile-top deforma-
tions are not large, but they are significant if the percent differences are
considered. The differences would be larger for larger diameter piles or
longer piles, or if loads are to exceed the working loads.

Conclusion and Recommendations

88. The methods by Coyle and Reese (1966) and Vijayvergiya (1977b) have many limitations. They do not account for factors which affect the shapes of f-z curves, such as soil stiffness and L/D ratio. Additionally computed values of side friction are directly proportional to f_{max} , so the shapes of the curves are affected by errors in computing f_{max} . Therefore, the two methods are not recommended for use.

89. The methods by Kraft, Ray, and Kawaga (1981) and Heydinger and O'Neill (in preparation) are comparable. They both have theoretical basis and have been verified with comparisons from field tests. The expression for the Heydinger and O'Neill method comes from a general equation. Kraft, Ray, and Kawaga (1981) use a hyperbolic equation to represent the change of the shear modulus, which results in f-z curves with shapes that are hyperbolic. Both methods account for factors which affect the shapes of f-z curves. They are both sensitive to the stress-strain modulus that is input.

90. The recommendation is to use either the method by Kraft, Ray, and Kawaga (1981) or the method by Heydinger and O'Neill (in preparation). The computed curves are very similar. It has been shown (Heydinger and O'Neill, in preparation; and Kraft, Ray, and Kawaga 1981) that the two methods can be used to predict f-z curves very accurately if representative values of E_u are known. Further verifications should be made using data from other tests wherever possible in order to come to a better understanding of the methods and their use.

PART IV: ENGINEERING PROPERTIES OF SOILS

Introduction

91. The purpose of this section is to describe research on engineering properties of soil. Soil properties can be estimated by using correlations with soil plasticity or normalized soil testing. The concept of normalized soil properties has been found to be valid for many soils. The following findings were obtained from research on soil properties for general geotechnical purposes and not specifically for use in design of piles.

Correlations With Plasticity

Correlations for φ'

92. Correlations for the effective angle of internal friction have been proposed by a number of investigators for normally consolidated clays. Figure 27, obtained from NAVFAC DM-7 (1979), shows the results reported by Bjerrum and Simons (1960). The true angle of internal friction, φr , is
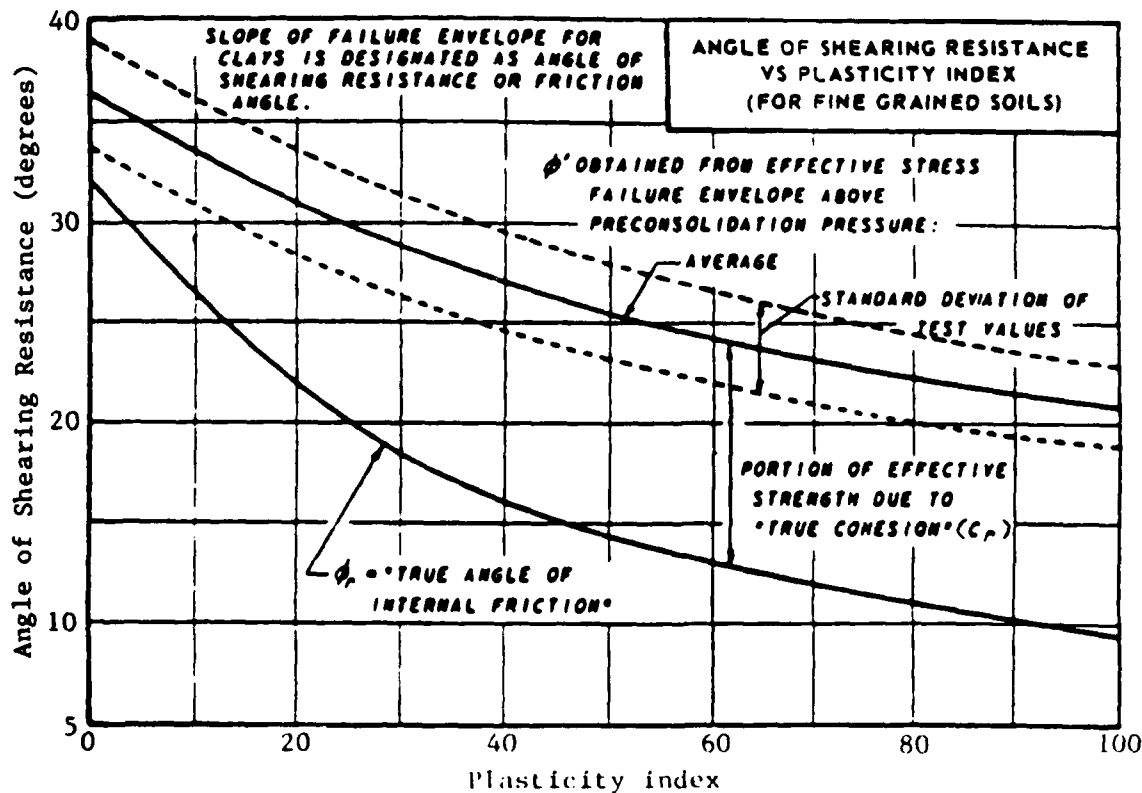
Figure 27. Correlation for φ' (NAVFAC DM-7)

53

determined from the deviator stress from samples with the same water contents. The curve for the effective friction angle, ϕ', was obtained from drained tests and from undrained tests with pore pressure measurements. For the undrained tests, ϕ' was determined using the maximum value of the ratio of the maximum stress to the minimum stress, σ_1'/σ_3', as the failure criterion.

93. Mayne (1980) reported the following equation for ϕ' for both normally and overconsolidated clays based on the plasticity index, PI , and the liquid limit, LL

$$\sin \phi' = 0.656 - 0.409 \frac{PI}{LL} \tag{32}$$

The correlation coefficient for Equation 32 is 0.583. Figure 28 shows the total friction angle obtained from consolidated-undrained triaxial tests, ϕ_{cu} , for marine soils. Based on these findings, it is apparent that the effective friction angle correlates poorly with index properties.
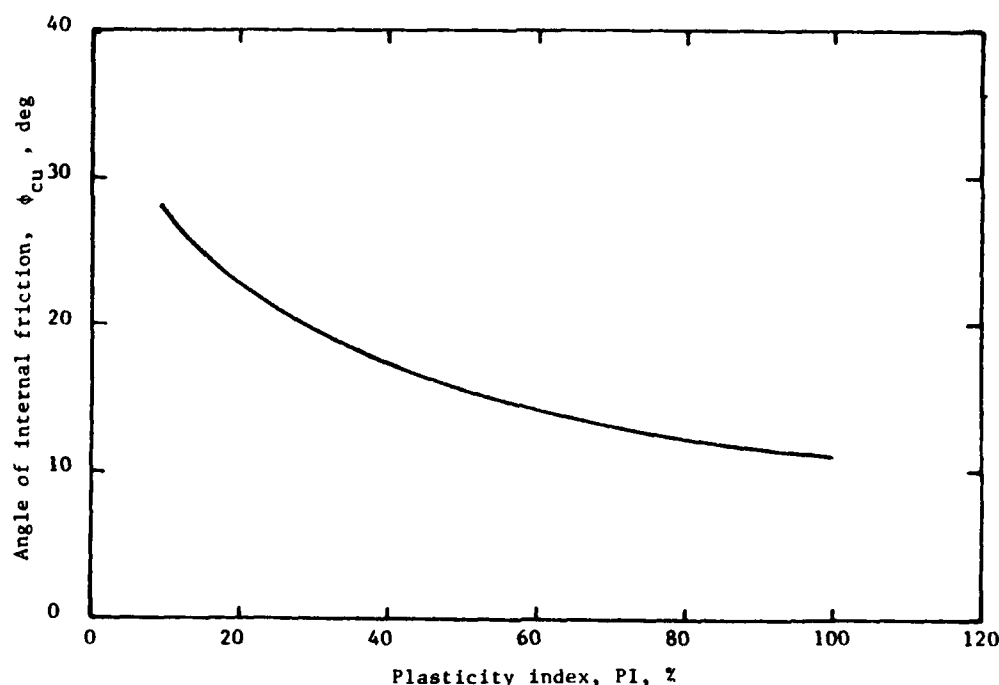
Figure 28.   Correlation for ϕ_{cu}(Vijayvergiya 1977b)

Correlations for K_o

94. The ratio of the horizontal effective stress to the vertical effective stress, K_o , is dependent on soil plasticity and stress history. Figure 29, from Ladd et al. (1977), indicates a general trend for K_o as a
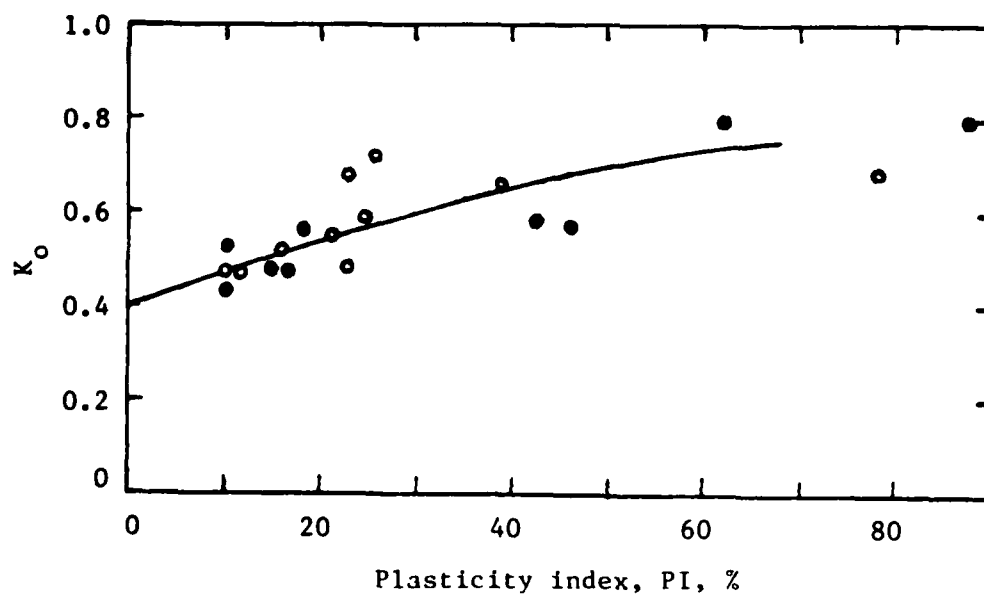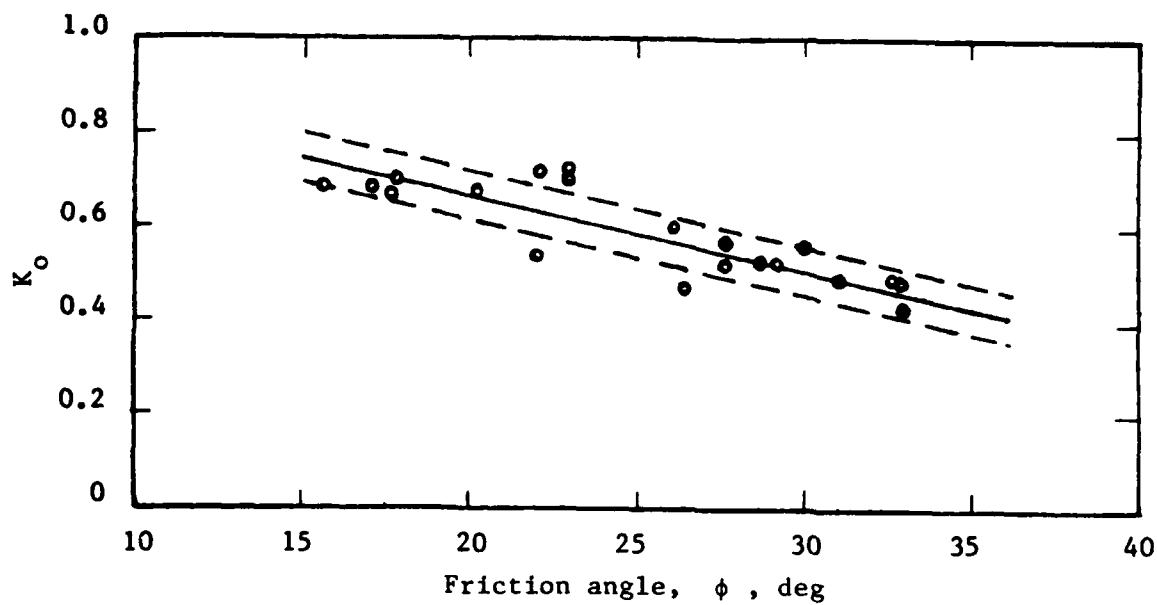
Figure 29. Correlations for K_O for normally
consolidated soils (Ladd et al. 1977)

function of plasticity index and ϕ' for normally consolidated soils. The following equation by Alpan (1967) gives K_O in terms of plasticity for normally consolidated clays.

$$K_O = 0.19 + 0.233 \log PI(\%) \tag{33}$$

95. An expression for the ratio of K_O for overconsolidated soils, $(K_O)_{oc}$, to the value for the soil if it was normally consolidated, $(K_O)_{nc}$, is given in terms of the OCR.

$$\frac{\left(K_O\right)_{oc}}{\left(K_O\right)_{nc}} = OCR^n \tag{34}$$

Figure 30 contains a curve for the parameter n as a function of PI for undisturbed soils (Vesic 1972). Figure 31 was proposed by Brooker and Ireland (1965). Vijayvergiya (1977a) computed Figure 32 using Figure 27 to compute ϕ and the following equation.

$$K_O = (1 - \sin \phi_{cu})(OCR)^{1/2} \tag{35}$$
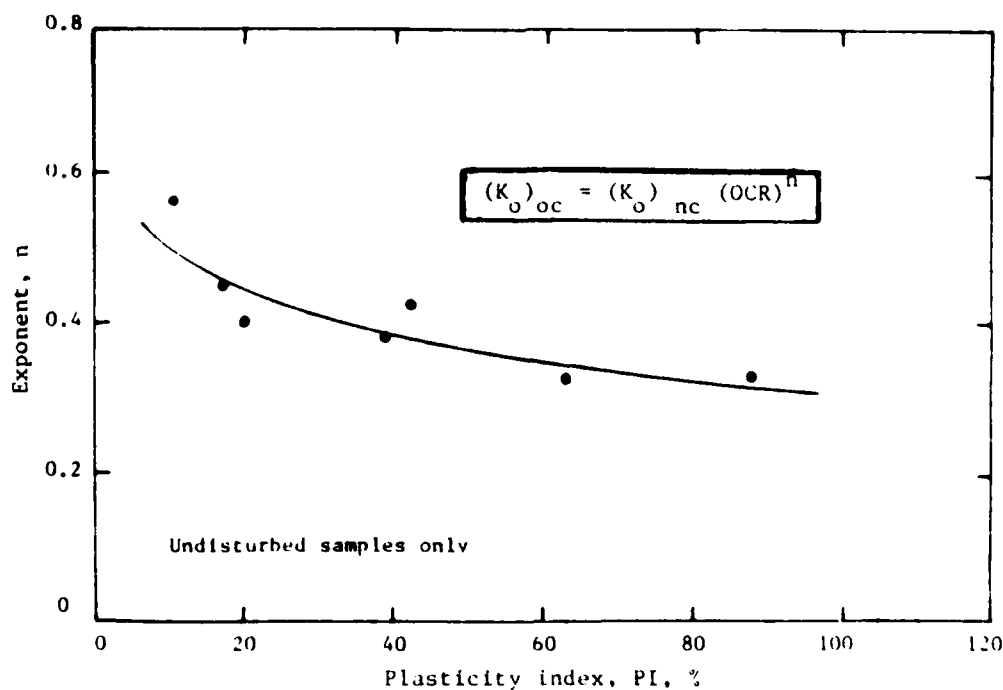
Figure 30. Exponent n versus PI (Vesic 1977)
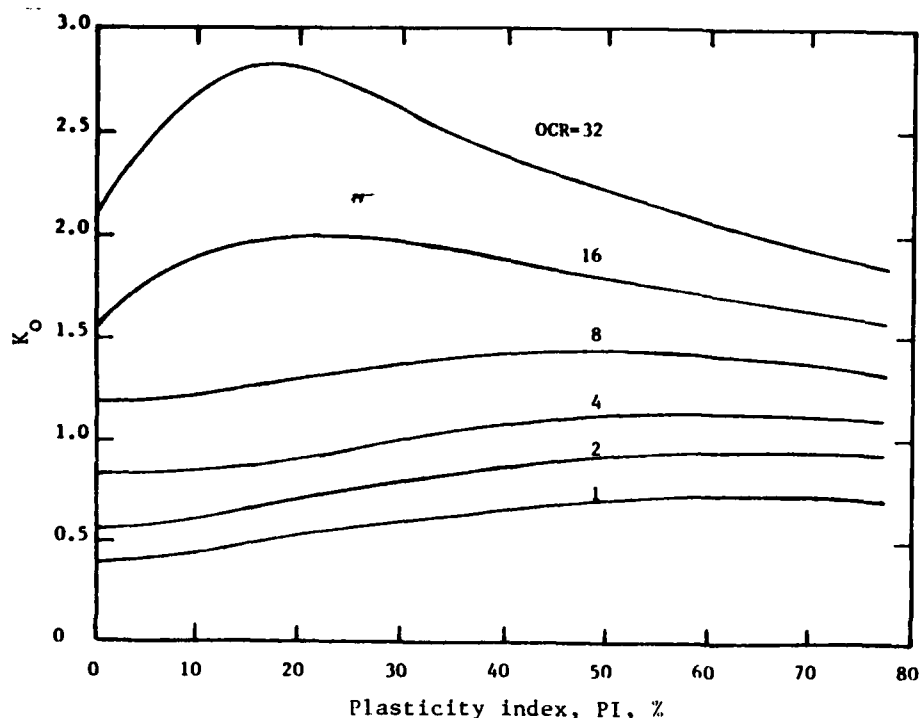
Figure 31. K_O as a function of PI and OCR
(Brooker and Ireland 1965)

The figures and equations indicate that K_O increases with increasing plasticity for both normally and overconsolidated soils, and that K_O increases with increasing OCR .

96. In addition to the previous recommendations, a statistical study by Mayne and Kulhawy (1982) has also been reported. The best relationship for K_O for normally consolidated clays was given as

$$\left(K_o\right)_{nc} = 1 - 0.987 \sin \phi'$$ (36)

The correlation coefficient for Equation 36 is 0.854. The authors also attempted to correlate $(K_o)_{nc}$ with plasticity and other index properties but concluded that no good relationships existed. Mayne and Kulhawy (1982) also recommended K_O for overconsolidated clays.

$$\left(K_o\right)_{oc} = (1 - \sin \phi')OCR^{\sin \phi'}$$ (37)
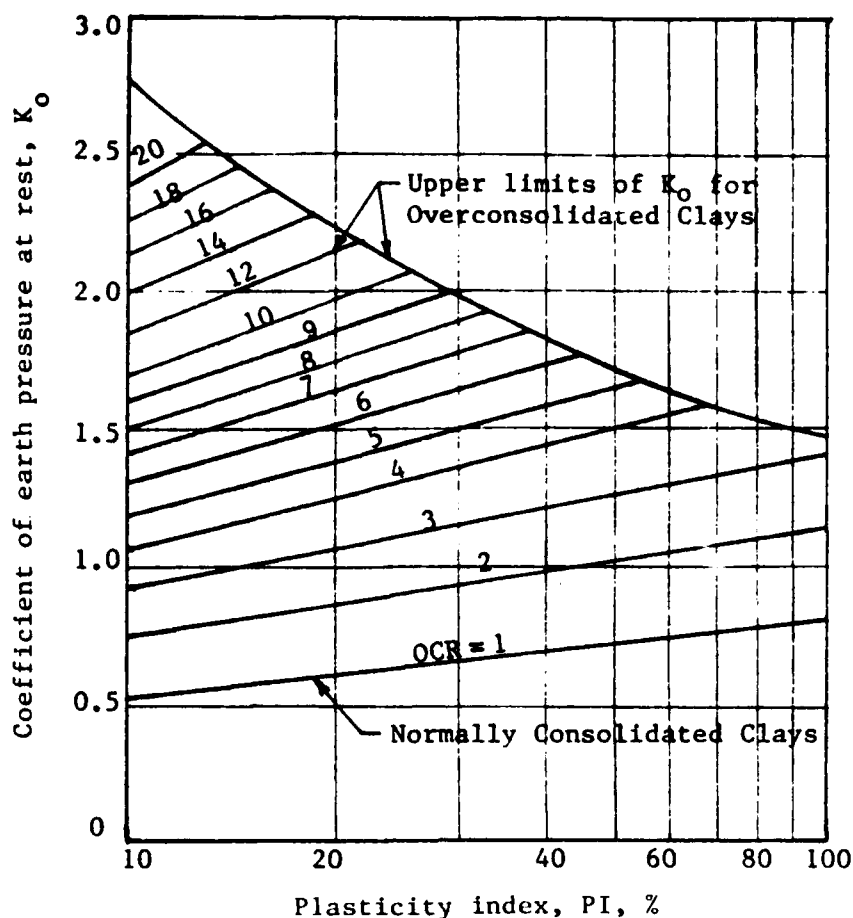
Figure 32. K_o as a function of PI and OCR
(Vijayvergiya 1977a)

Correlations for un-
drained shear strength

97. Relationships have been proposed for the undrained shear strength normalized by the vertical effective stress, s_u/σ_v', as a function of plasticity. Using the results of vane shear and unconfined compression tests, Bjerrum and Simons (1960) have shown in Figure 33 that the ratio s_u/p, (where $p = \sigma_v'$), increases as the PI increases for normally consolidated marine clays. They also showed in Figure 34 that the ratio decreases as the liquidity index increases, and stated that values of the ratio would be higher for freshwater soils. Figure 35, from NaKase and Kamei (1983) indicates relationships for the ratios for compression and extension tests for freshwater soils. Curves were determined for normally consolidated freshwater soils from the results of triaxial compression (TC) and direct simple shear tests (DSS) as shown in Figure 36. Mayne (1980) proposed the following relationship for normally consolidated clays.

58
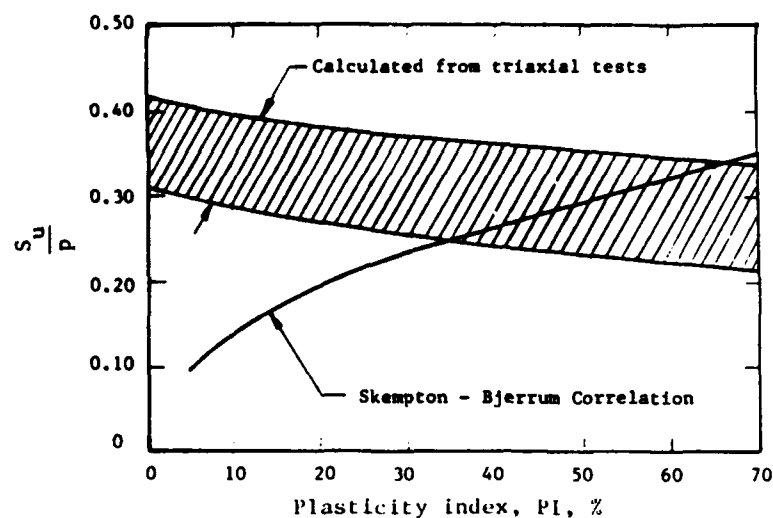
Figure 33. s_u/p versus PI

(Bjerrum and Simons 1960)
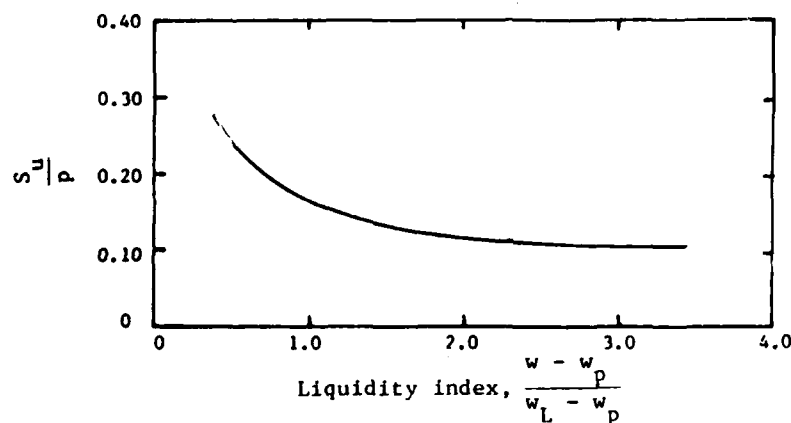
Figure 34. s_u/p versus LI

(Bjerrum and Simons 1960)

$$\frac{s_u}{\sigma'_v} = 0.642 \sin \phi' + 0.031 \tag{38}$$

The correlation coefficient for Equation 38 is 0.722. The trend is for s_u/σ'_v to increase with increasing plasticity and to decrease as the water content, i.e., LI increases.

Normalized Soil Testing

98. The results presented for normalized testing are based on the
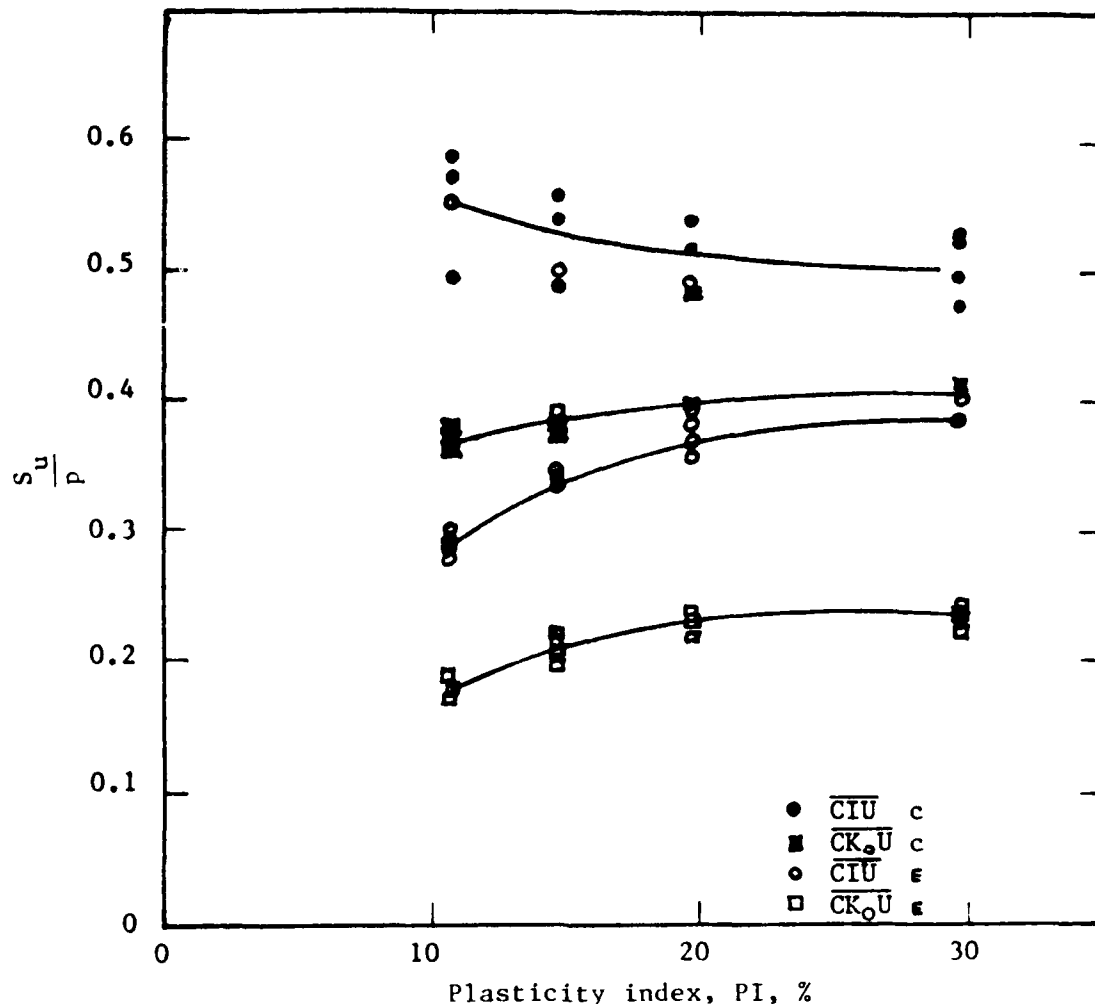
Figure 35. s_u/p versus PI
(NaKase and Kamei 1983)

normalized soils properties (NSP) concept and the stress history and normalized soil engineering properties (SHANSEP) method of design (Ladd and Foott 1974). The hypothesis is that the effects of soil overconsolidation can be duplicated in a laboratory by consolidating samples to pressures greater than any previously encountered. After the samples are allowed to swell back to lower pressures, they are then sheared to failure. The testing procedure is an attempt to overcome the effects of soil disturbance due to sampling. Soils that are sensitive or that are naturally cemented due to thixotropic effects would not behave according to normalized behavior.

Normalized undrained shear strength

99. The normalized undrained shear strength is dependent on the OCR
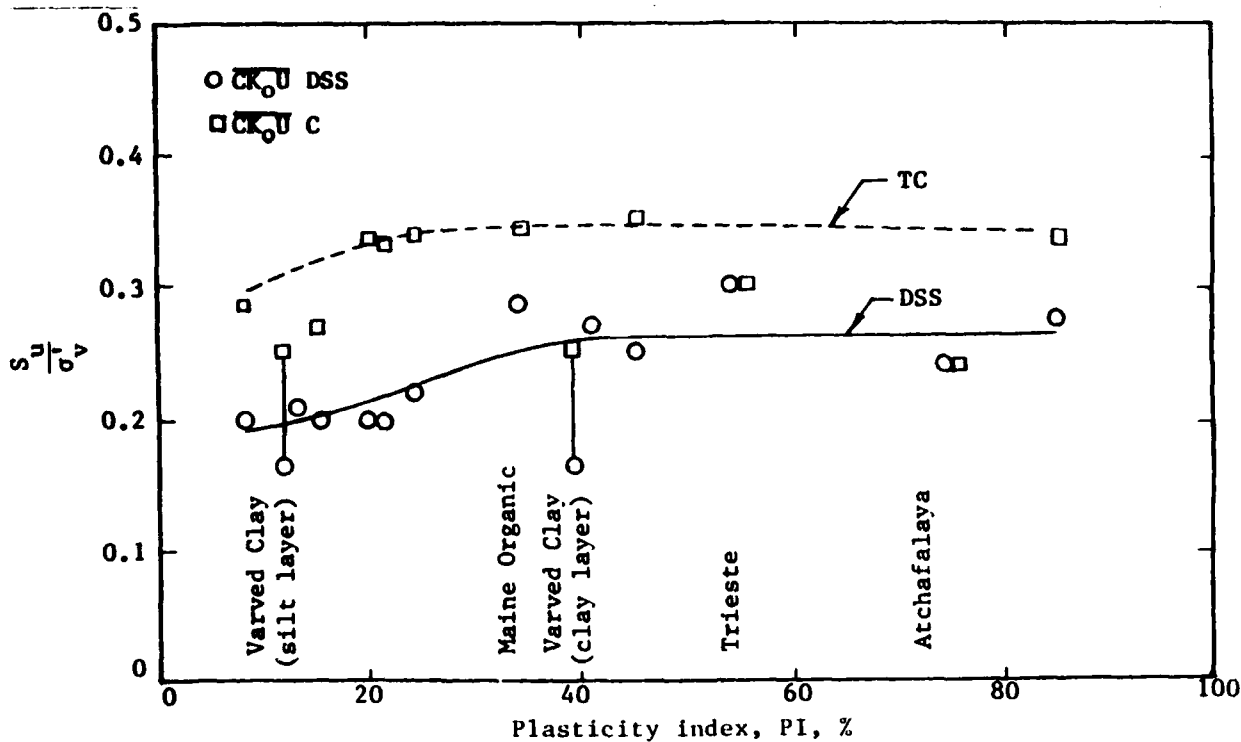
Figure 36. s_u/p versus PI for normally
consolidated soil (Gardner 1977)

of the soil (Simons 1960, Skempton 1957). By consolidating samples and then allowing them to swell back, soils with known OCR's are obtained. The OCR is then defined as the ratio of maximum vertical consolidation pressure, σ'_{vm} , to the vertical consolidation pressure after swelling, σ'_v . Typical curves of s_u/σ'_v versus the log of OCR , shown in Figure 37, indicate that the ratio increases similarly for soils of different plasticity (Vijayvergiya 1977a). There is, however, no definite relationship between PI and the ratio. By plotting $\frac{s_u/\sigma'_v}{oc}$ $\frac{s_u/\sigma'_v}{nc}$ versus the log of OCR , Vijayvergiya

(1977a) obtained a range of values that can be used to estimate s_u/σ'_v for overconsolidated soils as shown in Figure 38.

100. Expressions for s_u/σ'_v have been obtained for overconsolidated soils. Gardner (1977) recommended the following equation for CIU triaxial testing on silty clays with PI = 16 ± 15 .

61

$$\frac{s_u}{\sigma'_v} = (0.41 \pm 0.06)OCR^{0.67} \tag{39}$$

Researchers in Japan (Hanzawa 1977, Hanzawa and Kishida 1982, NaKase and Kamei 1983) recommended the following equation obtained from K_o consolidation tests (CK_oU).

$$\frac{s_u}{\sigma'_v} = (0.355)OCR \tag{40}$$
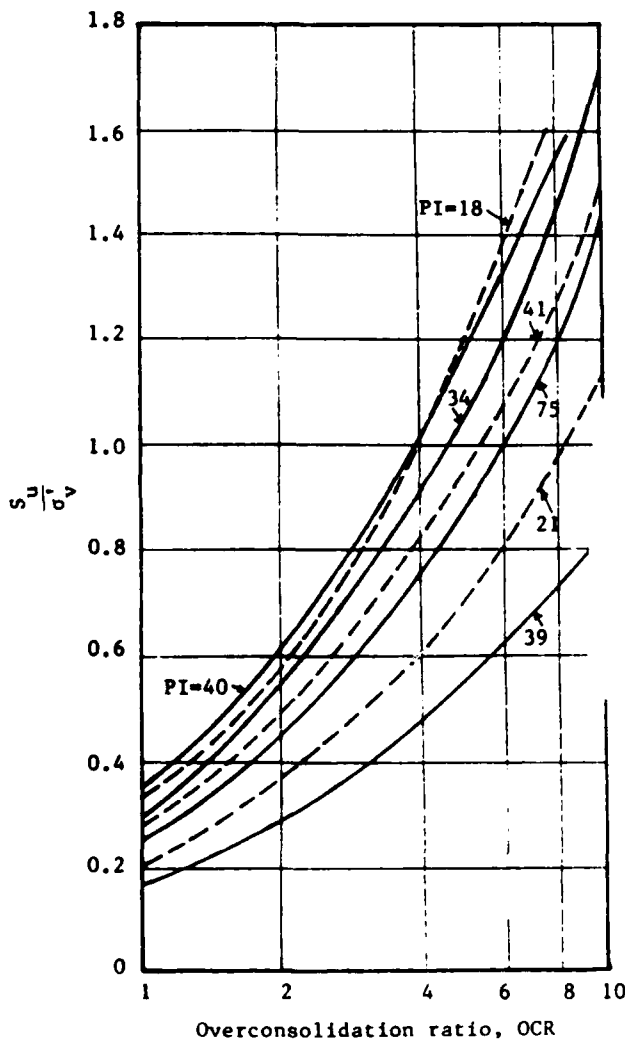
Figure 37. s_u/σ'_v versus OCR (Vijayvergiya 1977a)

101. Researchers have reported that soil consolidated to high pressures in the laboratory experiences an increase in strength with time (Bjerrum and Lo 1963, Leroueil et al. 1979, Tavenas and Leroueil 1977). The explanation is that soils subjected to thixotropic or secondary consolidation effects will gain strength if permitted to age. Reductions of shear strength of 30 percent for young clays, as compared to old clays, have been documented. The implication is that the normalized testing procedure would result in reductions in shear strength.

Normalized undrained modulus

102. Undrained soil moduli have been normalized by the undrained shear strength and the vertical effective consolidating pressures. The ratios are dependent on the OCR of the soil and on plasticity. The ratios also depend on the level of shear stress that is used to compute the undrained modulus. The initial modulus, taken at very low strain, is recommended for predicting f-z curves and other problems.
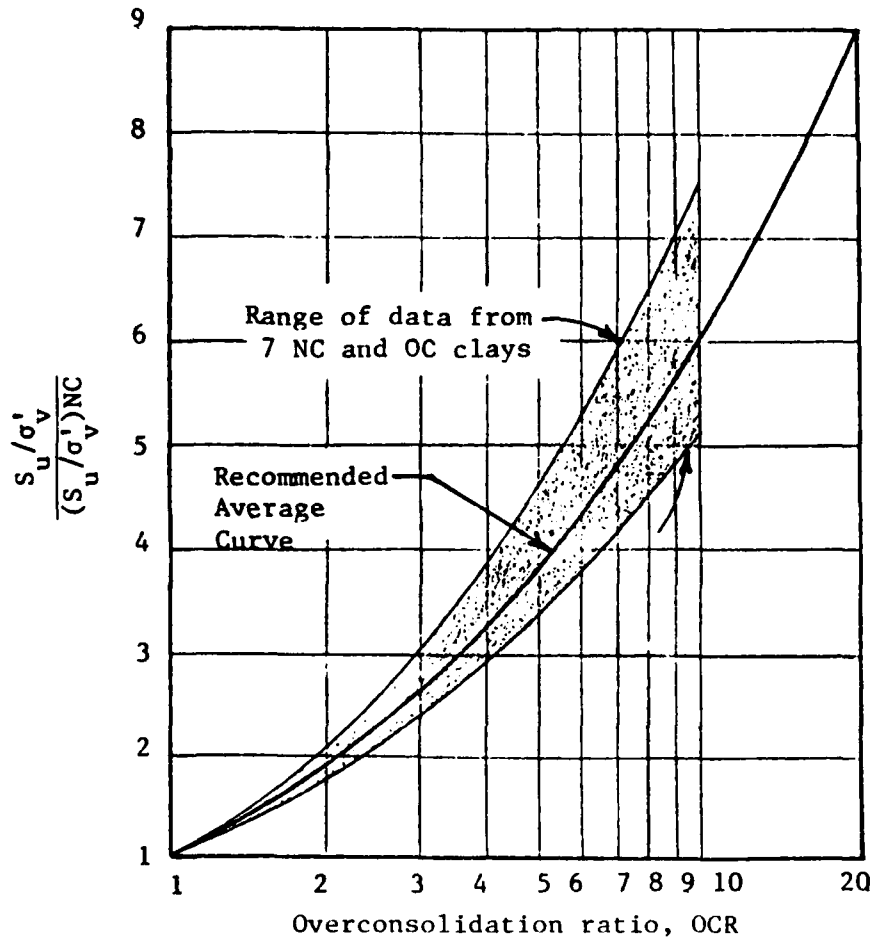
Figure 38. $\left(s_u/\sigma_v'\right)_{oc}\left(s_u/\sigma_v'\right)_{nc}$ versus OCR (Vijayvergiya 1977a)

103. The ratio E_u/s_u has been found to be very sensitive to OCR and plasticity. The ratio decreases appreciably as both OCR and plasticity increase. Values ranging from 1,200 to 1,500 have been measured in laboratory testing for soils with PI less than 30 percent (D'Appolonia, Poulos, and Ladd 1971). The following equation, based on analysis of a number of tests, was recommended from the initial shear modulus, G_0 (Hara et al. 1974)

$$G_0 = 487s_u^{0.928} \ (\text{kg/cm}^2) \tag{41}$$

An approximation is $G_0/s_u = 500$. Values of E_u/s_u as low as 100 have been reported for highly plastic and organic soils (D'Appolonia, Poulos, and Ladd 1971).

104. The ratio E_u/σ_v' is not very sensitive to overconsolidation and plasticity. Amarasinghe and Parry (1975) reported that the ratio did not change much. Yudbir and Varadarajan (1974) reported that the ratio increases once the OCR exceeds a value of 100. The trend for ratios of E_u/σ_v' is that they decrease somewhat with increasing plasticity. Typical values of the ratio are in the range of 100 to 400.

Recommendations

105. Some specific recommendations for estimating the engineering properties of soils are given, followed by examples of their use. As can be seen in the previous discussion, the soil properties do not correlate very well. Therefore, it is emphasized that the recommendations are intended only to be used for initial estimates or as an aid in interpreting soils data. They should be used for final design only if it is not practical to obtain quality triaxial testing results. Thus, it is still necessary to conduct extensive laboratory tests for large projects.

106. The recommendations are based on the reported statistical analyses and on the results of normalized testing. The recommendation for estimating the effective angle of internal friction is to use Equation 32. This correlation, although not very good, is the best correlation available. The two correlations for K_o that can be used for normally consolidated soils are given in Equations 33 and 36, depending on the information that is available. Equation 35 or 37 can be used to estimate K_o for overconsolidated soils.

107. The undrained shear strength is estimated from normalized parameters. For normally consolidated soils, the ratio s_u/σ_v' is obtained from Equation 38, or $s_u/\sigma_v' = 0.35$ can be used. The ratio s_u/σ_v' can be obtained for overconsolidated soils using an equation that is similar to Equation 39, where the quantity $0.41 + 0.06$ is equal to the value of the ratio for normally consolidated soils. By plotting, for example, the curves in Figure 37 using the logarithm of s_u/σ_v' versus the logarithm of OCR , a set of lines that are approximately parallel is obtained. The slope of the lines is the exponent of OCR in Equation 39. The average slope of the lines in Figure 37 is approximately 0.73. Therefore, the following equation is recommended

$$\frac{s_u}{\sigma_v'} = \left(\frac{s_u}{\sigma_v'}\right)_{nc} OCR^{0.70} \qquad (42)$$

The undrained shear strength could possibly be overestimated using Equation 40.

108. The undrained soil modulus is estimated using E_u/s_u or E_u/σ_v', where E_u is the initial modulus or the slope of the initial tangent to the stress-strain curves. The OCR and soil plasticity both have an effect on the values of the two ratios, with the ratios tending to decrease as the OCR and the PI increase. There appears to be no consistent trend; therefore, no relationships are given in this report. The range of values of E_u/s_u is typically 600 to 1,500. The range of values of E_u/σ_v' is approximately 100 to 400. The previous analyses with f-z curves indicate that more accurate f-z curves are obtained if the higher values in the ranges of values are used for insensitive soils, and if lower values are used for slightly sensitive and sensitive soils.

Example of predic-
tion of soil properties

109. The first example of prediction of soil properties was made for soil at the SFBM site (Kirby and Rousell 1979 and 1980). The soil is a slightly sensitive, normally consolidated clay of high plasticity. The computed vertical effective stress for a depth of 20 ft is 944 psf. The effective angle of internal friction was computed using Equation 32 with PI = 37 and LL = 93 . The computed value is 29.5 deg, as compared to an average value of 34 deg determined from triaxial testing. Estimated values of K_o equal to 0.56 and 0.51 were obtained using Equations 33 and 36, respectively, using 29.5 deg for the effective friction angle. The investigators for the pile test estimated $K_o = 0.49$. The ratio of s_u/σ_v' was estimated to be 0.346 using Equation 38 as compared to 0.35 which was determined from triaxial testing. The ratio $E_u/s_u = 600$ that was recommended by the investigators of the site corresponds to $E_u/\sigma_v' = 208$. Using the estimated soil properties, predicted f-z curves similar to those shown in Figure 21 would be obtained.

110. The second example of predictions was for the UHCC site (O'Neill, Hawkins, and Mahar 1981). The soil at the site is an insensitive, highly overconsolidated clay of high plasticity. The effective vertical stress at a depth of 20 ft was computed to be 1,912 psf. The effective angle of internal

friction equal to 24.8 deg was computed using Equation 32 with $PI = 40$ and $LL = 68$. An effective angle equal to 24 deg was determined from triaxial tests. K_o equal to 1.42 and 1.23 was computed using Equations 35 and 37. Values of K_o as low as 1 were obtained from laboratory tests, and values of K_o as high as 2.5 were obtained from pressuremeter tests at the site.

111. In order to obtain s_u/σ_v' for the overconsolidated soil, $s_u/\sigma_v' = 0.30$ was estimated for a normally consolidated soil using Equation 38. $s_u/\sigma_v' = 1.05$ was then computed using Equation 42. The estimated undrained shear strength would then be 2,008 psf as compared to 1,700 which was determined from normalized testing at the site and 2,000 which was determined from unconsolidated, undrained triaxial shear tests. The undrained soil modulus was estimated using $E_u/s_u = 1,000$, which corresponds to $E_u = 2,008,000$ psf or 13,944 psi. Values of E_u equal to 3,000, 10,000, and 40,000 psi were obtained from normalized soil testing, pressuremeter testing, and crosshole tests. The computed value of E_u/σ_v' is 1,050. Predicted f-z curves similar to the curves in Figure 20 would be obtained using the estimated soil properties.

REFERENCES

Alpan, I. 1967. "The Empirical Evaluation of the Coefficient K_o and K_{or}," Soil and Foundation, Vol VII, No. 1, pp 31-40.

Amarasinghe, S. R., and Parry, R. H. G. 1975 (Dec). "Anisotrophy in Heavily Overconsolidated Kaolin," Journal, Geotechnical Engineering Division, American Society of Civil Engineers, Vol 101, No. GT12, pp 1277-1293.

American Petroleum Institute. 1978. "Recommended Practice for Planning, Designing and Constructing Offshore Platforms," API RP 2A, 9th ed.

Baguelin, F., and Frank, R. 1980. "Theoretical Studies of Piles Using the Finite Element Method," Conference on Numerical Methods in Offshore Piling, Institute of Civil Engineers, London, pp 83-91.

Baguelin, F., Frank, R., and Jezequel, J. F. 1982 (Apr). "Parameters for Friction Piles in Marine Soils," Proceedings, Second International Conference on Numerical Methods in Offshore Piling, Austin, Tex.

Bjerrum, L., and Lo, K. Y. 1963. "Effect of Aging on the Shear Strength Properties of a Normally Consolidated Clay," Geotechnique, Vol 13, pp 147-157.

Bjerrum, L., and Simons, N. E. 1960. "Comparison of Shear Strength Characteristics of Normally Consolidated Clays," Proceedings, Research Conference on Shear Strength of Cohesive Soils, American Society of Civil Engineers, University of Colorado, pp 711-726.

Blanchet, R., Tavenas, F., and Garneau, R. 1980 (May). "Behavior of Friction Piles in Soft Sensitive Clays," Canadian Geotechnical Journal, pp 203-224.

Brooker, E. W., and Ireland, H. O. 1965. "Earth Pressures at Rest Related to Stress History," Canadian Geotechnical Journal, Vol 11, No. 1.

Carter, J. P., Randolph, M. F., and Wroth, C. P. 1979. "Stress and Pore Pressure Changes in Clay During and After the Expansion of a Cylindrical Cavity," International Journal for Numerical and Analytical Methods in Geomechanics, Vol 3, pp 305-322.

Coyle, H. M., and Reese, L. C. 1966. "Load Transfer for Axially Loaded Piles in Clay," Journal, Soil Mechanics and Foundations Division, American Society of Civil Engineers, Vol 92, No. SM2, pp 1-26.

D'Appolonia, D. J., Poulos, H. G., and Ladd, C. C. 1971 (Oct). "Initial Settlement of Structures on Clay," Journal, Soil Mechanics and Foundations Division, American Society of Civil Engineers, Vol 97, No. SM10, pp 1359-1377.

D'Appolonia, E., and Romualdi, J. P. 1963. "Load Transfer in End-Bearing Steel H-Piles," Journal, Soil Mechanics and Foundations Division, American Society of Civil Engineers, Vol 89, No. SM2, pp 1-25.

Dennis, N. D., Jr., and Olson, R. E. 1983 (Apr). "Axial Capacity of Steel Pipe Piles in Clay," Proceedings, Conference on Geotechnical Practice in Offshore Engineering, University of Texas, Austin, Tex., pp 370-388.

Esrig, M. I., et al. 1977. "Initial Development of a General Effective Stress Method for the Prediction of Axial Capacity for Driven Piles in Clay," Proceedings, Ninth Offshore Technology Conference, Houston, Tex., Paper No. 2943, pp 495-506.

Esrig, M. I., and Kirby, R. C. 1979. "Advances in General Effective Stress Method for the Prediction of Axial Capacity for Driven Piles in Clay," Proceedings, 11th Offshore Technology Conference, Houston, Tex., Vol 1, Paper No. 3406, pp 437-448.

Gardner, W. S. 1977. "Soil Property Characterization in Geotechnical Engineering Practice," Geotechnical/Environmental Bulletin, Vol X, No. 2, Woodward Clyde Consultants, San Francisco, Calif.

Hanzawa, H. 1977 (Dec). "Field and Laboratory Behavior of Khor Al-Zubair Clay, Iraq," Soils and Foundations, Vols 17 and 22, No. 4 pp 17-30.

Hanzawa, H., and Kishida, T. 1982 (Jun). "Determination of In Situ Undrained Strength of Soft Clay Deposits," Soils and Foundations, Vol 22, No. 2, pp 1-14.

Hara, A., et al. 1974 (Sep). "Shear Modulus and Shear Strength of Cohesive Soils," Soils and Foundations, Vol 14, No. 3, pp 1-12.

Heydinger, A. G., and O'Neill, M. W. "Analysis of Axial Pile-Soil Interaction in Clay" (in preparation), International Journal for Numerical and Analytical Methods in Geomechanics.

Kavvadas, M., and Baligh, M. M. 1982 (Aug). "Nonlinear Consolidation Analyses Around Pile Shafts," Proceedings, Third International Conference on the Behavior of Offshore Structures, Vol 2, pp 338-347.

Kirby, R. C., and Esrig, M. I. 1979. "Further Development of a General Effective Stress Method for Prediction of Axial Capacity for Driven Piles in Clay," Proceedings, Conference on Recent Development in the Design and Construction of Piles, Institute of Civil Engineers, London.

Kirby, R. C., Esrig, M. I., and Murphy, B. S. 1983 (Apr). "General Effective Stress Method for Piles in Clay," Proceedings, Conference on Geotechnical Practice in Offshore Engineering, University of Texas, Austin, Tex., pp 457-498.

Kirby, R. C., and Roussel, G. 1979 and 1980. "Report on ESACC Project Field Model Pile Load Test, Hamilton Air Force Base Test Site, Novato, California," four reports prepared for Amoco Production Company by Woodward-Clyde Consultants, Clifton, N. J.

Kirby, R. C., and Wroth, C. P. 1977. "Applications of Critical State Soil Mechanics to the Prediction of Axial Capacity for Driven Piles," Proceedings, Ninth Offshore Technology Conference, Houston, Tex., Vol 3, Paper No. 2942, pp 483-494.

Konrad, J. M. 1977. Contribution Au Calcul de Frottement Latéral des Pieux Flottants Fonces dans des Argiles Molles et Sensibles, M.S. Thesis, University of Laval, Quebec, Canada.

Kraft, L. M., Jr. 1982 (Nov). "Effective Stress Capacity Model for Piles in Clay," Journal, Geotechnical Engineering Division, American Society of Civil Engineers, Vol 198, No. GT11, pp 1387-1404.

Kraft, L. M., Jr., Focht, J. A., and Amarasinghe, S. R. 1981 (Nov). "Friction Capacity of Piles Driven into Clay," Journal, Geotechnical Engineering Division, American Society of Civil Engineers, Vol 107, No. GT11, pp 1521-1541.

Kraft, L. M., Jr., Ray, R. P., and Kagawa, T. 1981 (Nov). "Theoretical t-z Curves," Journal, Geotechnical Engineering Division, American Society of Civil Engineers, Vol 107, No. GT11, pp 1543-1561.

Ladd, C. C., and Foott, R. 1974. "New Design Procedure for Stability of Soft Clays," Journal, Geotechnical Engineering Division, American Society of Civil Engineers, Vol 100, No. GT7, pp 763-786.

Ladd, C. C., et al. 1977. "State of the Art Report on Stress-Deformation and Strength Characteristics," Proceedings, Ninth International Conference on Soil Mechanics and Foundation Engineering, Tokyo, Vol 2, pp 421-494.

Leifer, S. A., Kirby, R. C., and Esrig, M. I. 1979. "Effects of Radial Variation of Material Properties on Stress Changes Due to Consolidation Around a Driven Pile," Proceedings, Conference on Numerical Methods in Offshore Piling, Institute of Civil Engineers, London, pp 129-135.

Leroueil, S. et al. 1979 (Jun). "Behavior and Destructured Natural Clays," Journal, Geotechnical Engineering Division, American Society of Civil Engineers, Vol 105, No. GT6, pp 759-778.

Mayne, P. W. 1980. "Cam-Clay Predictions of Undrained Shear Strength," Journal, Geotechnical Engineering Division, American Society of Civil Engineers, Vol 106, GT 11, pp 1219-1242.

Mayne, P. W., and Kulhawy, F. H. 1982 (Jun). "K-OCR Relationships in Soil," Journal, Geotechnical Engineering Division, American Society of Civil Engineers, Vol 108, No. GT6, pp 851-872.

Meyerhof, G. G. 1976. "Bearing Capacity and Settlement of Pile Foundations," Journal, Geotechnical Engineering Division, American Society of Civil Engineers, Vol 102, No. GT3, pp 197-228.

Miller, T. W., Murff, J. D., and Kraft, L. M., Jr. 1978. "Critical State Soil Mechanics Model of Soil Consolidation Stresses Around a Driven Pile," Proceedings, Tenth Offshore Technology Conference, Vol 13, Paper No. 3307, pp 2237-2242.

Mosher, R. 1984 (Jan). "Load-Transfer Criteria for Numerical Analysis of Axially Loaded Piles in Sand," Technical Report K-84-1, US Army Engineer Waterways Experiment Station, Vicksburg, Miss.

NaKase, A., and Kamei, T. 1983 (Mar). "Undrained Shear Strength Anisotrophy of Normally Consolidated Cohesive Soils," Soils and Foundations, Japanese Society of Soil Mechanics and Foundation Engineering, Vol 23, No. 1, pp 91-101.

Naval Facilities Engineering Command. 1979 (Mar). "Design Manual-Soil Mechanics Foundations and Earth Structures," NAVFAC DM-7, Department of the Navy, Washington, DC.

O'Neill, M. W., Hawkins, R. A., and Mahar, L. J. 1981 (Mar). "Field Study of Pile Group Action," Report FHWA IRD-18/002, Federal Highway Administration, Office of Research and Development, Washington, DC.

Potts, D. M., and Martins, J. P. 1982 (Apr). "The Shaft Resistance of Driven Piles in Clay," Proceedings, Second International Conference on Numerical Methods in Offshore Piling, Austin, Tex.

Radhakrishnan, N., and Parker, F. P. 1975 (May). "Background Theory and Documentation of Five University of Texas Soil Structure Interaction Programs," Miscellaneous Paper K-75-2, US Army Engineer Waterways Experiment Station, Vicksburg, Miss.

Randolph, M. F., and Wroth, C. P. 1978 (Dec). "Analysis of Deformation of Vertically Loaded Piles," Journal, Geotechnical Engineering Division, American Society of Civil Engineers, Vol 104, No. GT2, pp 1465-1488.

_____. 1979. "An Analytical Solution for the Consolidation Around a Driven Pile," International Journal for Numerical and Analytical Methods in Geomechanics, Vol 3, pp 217-229.

Randolph, M. F., Carter, J. P., and Wroth, C. P. 1979. "Driven Piles in Clay--The Effects of Installation and Subsequent Consolidation," Geotechnique, Vol 29, No. 4, pp 301-327.

Roy, M. et al. 1981 (Jul). "Behavior of a Sensitive Clay During Pile Driving," Canadian Geotechnical Journal, Vol 18, pp 67-85.

Schofield, A. N., and Wroth, C. P. 1968. Critical State Soil Mechanics, McGraw-Hill, New York.

Shilstone Testing Laboratory. 1976 (Jul). "Test Pile Program Report, East Atchafalaya Basin Protection Levee."

Simons, N. E. 1960. "The Effect of Overconsolidation on the Shear Strength Characteristics of an Undisturbed Oslo Clay," Proceedings, Research Conference on Shear Strength of Cohesive Soils, American Society of Civil Engineers, Boulder, Colo., pp 747-763.

Skempton, A. W. 1957. "Discussion of Planning and Design of the New Hong Kong Airport," Proceedings, Institute of Civil Engineers, Vol VII.

Tavenas, F., and Leroueil, J. 1977. "Effects of Stresses and Time of Yielding of Clays," Proceedings, Ninth International Conference on Soil Mechanics and Foundation Engineering, Tokyo, Vol 1, pp 319-326.

Tomlinson, M. J. 1957. "The Adhesion of Piles Driven in Clay Soils," Proceedings, Fourth International Conference on Soil Mechnics and Foundation Engineering, Vol 2, pp 66-71.

_____. 1964. Foundation Design and Construction, Wiley, New York.

_____. 1971. "Some Effects of Pile Driving on Skin Friction," Proceedings, Institute of Civil Engineers Conference: Behavior of Piles, London, pp 107-114.

US Army Engineer District, New Orleans. 1977 (Nov). "Interpretation of Pile Load Testing at East Atchafalaya Basin Protection Levee."

Vesic, A. S. 1972. "Expansion of Cavities in Infinite Soil Mass," Journal, Soil Mechanics and Foundation Division, American Society of Civil Engineers, Vol 98, pp 265-290.

_____. 1977. "Design of Pile Foundations," National Cooperative Highway Research Program, Synthesis of Highway Practice No. 42, Transportation Research Board, Washington, DC.

Vijayvergiya, V. N. 1977a (May). "Friction Capacity of Driven Piles in Clay," Proceedings, Ninth Offshore Technology Conference, Paper No. OTC 2939, pp 465-474.

Vijayvergiya, V. N. 1977b. "Load-Movement Characteristics of Piles," Proceedings, Fourth Symposium of Waterway, Port, Coastal, and Ocean Division, American Society of Civil Engineers, Long Beach, Calif., Vol 2, pp 269-284.

Vijayvergiya, V. N., and Focht, J. A. 1972. "A New Way to Predict Capacity of Piles in Clay," Proceedings, Fourth Offshore Technology Conference, Houston, Tex., Vol 2, pp 865-874.

Wroth, C. P., Carter, J. P., and Randolph, M. F. 1979. "Stress Changes Around a Pile Driven into Cohesive Soil," Proceedings, Conference on Recent Developments in the Design and Construction of Piles, Institute of Civil Engineers, London, pp 163-182.

Yudbir and Varadarajan, A. 1974 (Dec). "Undrained Behavior of Overconsolidated Saturated Clays During Shear," Soils and Foundations, Japanese Society of Soil Mechanics and Foundation Engineering, Vol 14, No. 4, pp 1-12.

Table 1
Soil-Pile Adhesion for Piles (After Tomlinson 1964)

Pile Material	Unconfined Compressive Strength, psf	Pile-Soil Adhesion, psf
Concrete and timber	0 to 1,500	0 to 700
	1,500 to 3,000	700 to 1,000
	3,000 to 6,000	1,000 to 1,300
	Over 6,000	Over 1,300
Steel	0 to 1,500	0 to 700
	1,500 to 3,000	700 to 1,000
	3,000 to 6,000	1,000 to 1,200
	Over 6,000	Over 1,200

Table 2
Comparison of Side Shear for UHCC Test

Depth ft	Measured f_{max} psf	Computed f_{max}				
		α	β	λ	Equation 20	Equation 22
0						
	0	889	727	1,074	433	479
8						
	800	822	1,100	1,034	1,008	1,114
16						
	1,400	862	1,790	1,249	2,110	2,427
26						
	1,250	667	1,339	855	1,404	1,535
30						
	1,500	1,200	1,380	2,134	1,641	1,787
43						
$\dfrac{Q_s \text{ (Computed)}}{Q_s \text{ (Measured)}}$		0.83	1.14	1.24	1.22	1.36

Table 3
Comparison of Side Shear for SFBM Test

Depth ft	Measured f_{max} psf	Computed f_{max}				
		α	β	λ	Equation 20	Equation 22
0						
	250	300	186	209	123	115
12.5						
	250	325	344	333	246	229
17.5						
	260	375	399	378	288	268
22.5						
	375	425	457	422	332	309
27.5						
	475	475	520	466	379	353
32.5						
	500	525	584	510	425	396
37.5						
	475	575	632	548	460	428
40						
$\dfrac{Q_s \text{ (Computed)}}{Q_s \text{ (Measured)}}$		1.21	1.18	1.11	0.84	0.79

Table 4

Comparison of Side Shear for St. Alban Test

Depth ft	Measured f_{max} psf	Computed f_{max}				
		α	β	λ	Equation 20	Equation 22
0						
	0	0	52	45	0	0
4						
	325	235	213	227	193	205
11						
	325	300	288	310	268	285
18						
	325	385	350	403	336	357
25						
$\dfrac{Q_s \text{ (Computed)}}{Q_s \text{ (Measured)}}$		0.94	0.90	0.99	0.82	0.87

Table 5

Comparison of Side Shear for EABPL Test

Depth ft	Measured f_max psf	Computed f_max				
		α	β	λ	Equation 20	Equation 22
0	610	350	92	169	86	92
7	610	300	214	229	200	213
13	321	300	283	272	265	281
21	338	200	285	275	289	350
29	370	200	316	298	321	389
37	330	200	342	317	347	420
42	330	300	435	366	407	432
45	514	300	489	399	458	485
53	237	550	567	528	531	563
61	237	550	617	558	577	612
63	241	666	661	665	619	656
70						
$\dfrac{Q_s \text{ (Computed)}}{Q_s \text{ (Measured)}}$		1.09	1.17	1.13	1.12	1.24

Table 6

Computed f-z Curves

Method z in.	Coyle and Reese (1966) f psf	Vijay-vergiya (1977b) f psf	Heydinger and O'Neill (In Preparation f psf	Kraft, Ray, and Kagawa (1981) f psf	z in.
0.025	329	345	244	65	0.007
0.035	481	394	340	130	0.013
0.050	599	450	473	195	0.021
0.070	648	505	588	259	0.028
0.100	611	561	638	324	0.037
0.125	597	593	645	389	0.046
0.150	591	615	647	454	0.056
0.175	588	631	648	519	0.068
0.200	582	641	648	584	0.085
0.250	579	648	648	616	0.097

APPENDIX A: NOTATION

A	Cross-sectional area
A_s	Area of the pile surface
A_t	Cross-sectional area of pile tip
c_a	Pile-soil adhesion
c_m	Mean, undrained shear strength
$\bar{c}_u$	Average, undrained shear strength
CIU	Consolidated, isotropic, undrained triaxial testing
D	Pile diameter
E	Young's modulus of pile resistance
E_u	Undrained modulus of elasticity
E_{fz}	Slope of the initial tangent of curve f versus z/D
$\left(E_u\right)_{ave}$	Average undrained soil modulus for a soil stratum
f_{max}	Maximum side resistance
f-z curves	Predictive methods for computing capacity and shear transfer versus pile movement
F_c	Ratio of the undrained shear strength using unconsolidated undrained triaxial tests to the strengths obtained by other methods
F_L	Length correction factors
G	Undrained shear modulus
G_i	Initial shear modulus
G_o	Secant shear modulus
ID	Inside diameter
K	Correlation factor for pile length to diameter ratio for Heydinger and O'Neill method
K_o	Ratio of the horizontal effective stress to the vertical effective stress for the at-rest condition
L	Pile length
LI	Liquidity index
LL	Liquid limit
m	Shape parameter for Heydinger and O'Neill method

m_o	Intercept values for m
M	$(6 \sin \phi')/(3 - \sin \phi')$
N_c	Cohesive bearing factor
OD	Outside diameter
OCR	Overconsolidated ratio of the soil
P_a	Atmospheric pressure
PI	Plasticity index
Q_u	Total pile capacity
Q-z curve	Tip load-deformation behavior
r	Radial distance
r_m	Radial zone of influence
r_o	Radius of pile
R_f	Stress-strain curve-fitting constant
s_u	Undrained shear strength
$\left(s_u\right)_{cs}$	Undrained shear strength for soil at critical state
u^*	Vertical pile movement resulting in maximum side
UU	Unconsolidated, undrained triaxial testing
z_c	Critical pile movement
z_s	Vertical displacement at the pile surface
α	Ratio of pile-soil adhesion to undrained shear strength
β	Correlation factor for in situ vertical overburden pressure to side resistance along a pile
$(\Delta\sigma_{rc}/u_e)$	Change in effective radial stress divided by the excess pore pressure, u_e
π_3	Parameter relating pile stiffness to soil stiffness
σ'_m	Mean effective overburden pressure
σ'_v	Vertical consolidation pressure after swelling
σ'_{vm}	Maximum vertical consolidation pressure
σ'_1/σ'_3	Ratio of the maximum stress to the minimum stress
τ	Shear stress
τ_o	Soil shear stress at the pile surface

τ_{max}	Maximum shear stress mobilized at pile failure
ϕ_r	True angle of internal friction
ϕ'	Effective angle of internal friction
ϕ'_{cs}	Effective angle of friction for soil at the critical state
ϕ_{cu}	Consolidated, undrained triaxial tests
ϕ_{ss}	Angle of friction between pile and soil

END

7-87

DTIC